RECOIL PROTONS FROM MESON PHOTOPRODUCTION IN HYDROGEN AND DEUTERIUM

Thesis by

William Rodman Smythe

In Partial Fulfillment of the Requirements

for the Degree of

Doctor of Philosophy

California Institute of Technology

Pasadena, California

1957

ACKNOWLEDGEMENTS

Dr. Alvin V. Tollestrup suggested and supervised this experiment, and his advice, suggestions and discussions were very helpful in its performance and subsequent analysis. The experimental work on the Cal Tech Synchrotron was performed during a period of eight weeks in the summer of 1954 jointly with Mr. Robert M. Worlock, who also made contributions to the analysis.

Dr. Robert F. Christy, Dr. James C. Keck, Dr. Matthew Sands, and Dr. Robert L. Walker have been helpful consultants on various occasions. The author appreciates the courtesy of the ElectroData Corporation in allowing him to attend their two weeks coding course. He would also like to thank the Jet Propulsion Laboratory and Mr. Max J. Seamons for cooperation in the use of the J. P. L. Datatron computer. Dr. Solomon Gartenhaus of Stanford University sent us a preprint of his paper (7) which proved quite useful.

The interest, assistance and encouragement of Dr. Robert F. Bacher throughout the author's graduate residence have been very valuable. The entire synchrotron staff, including the graduate students, has contributed in various ways to the success of this project. I am grateful to my wife, Carol, who has been a source of encouragement as well as a direct help in the typing of the first draft of this thesis, and to my father, Dr. W. R. Smythe, for proofreading the first draft. The partial

financial support of the United States Atomic Energy Commission is appreciated.

ABSTRACT

The spectrum of photoprotons produced by 500 mev bremsstrahlung on hydrogen and deuterium has been measured at laboratory angles of 29.7^{o}, 41.2^{o}, and 51.8^{o}. The protons were detected by a three scintillation counter telescope. The first counters were in coincidence and the third was in anticoincidence. Absorbers placed in front of and between the counters fixed the range of the particles observed, and the specific ionization in the front counter identified the protons. From the hydrogen data the π^{o} cross section of hydrogen was obtained, which agrees with the results of Oakley and Walker (1). The contribution of the deuterium photodisintegration reaction was subtracted from the deuterium counting rate and the deuterium to hydrogen ratio of recoil protons from meson production was obtained. This ratio is also calculated from the deuterium π^{-} and hydrogen π^{o} cross sections, by means of the spectator model of the deuteron (photons interact with only one of the deuterium nucleons). The initial motion of the target nucleon in the deuteron is taken into account. The calculated ratio is in agreement with the measured ratio if one corrects the spectator model for the fact that 11% of the mesons produced in deuterium are reabsorbed producing photodisintegration. The method of analysis developed is applied to other deuterium photomeson experiments.

TABLE OF CONTENTS

I. INTRODUCTION

In this experiment hydrogen and deuterium were bombarded with 500 mev bremsstrahlung and recoil protons were observed with a scintillation counter system. The observed particle was required to stop between the second and third scintillation counters, which defined the particle's range. The particle was identified as a proton by its specific ionization in the first counter.

The hydrogen data was analyzed to obtain the cross section for neutral pion photoproduction from hydrogen. This measurement of the cross section agrees with the measurement made by Oakley and Walker (1), who used a magnet to analyze the recoil protons.

After the completion of a hydrogen run the target was evacuated (for background runs) and then filled with deuterium. The measurements were repeated with the same geometry, obtaining deuterium to hydrogen photoproton ratios which were independent of the absolute calibration of the ion chamber beam monitor. Since the deuteron is rather loosely bound, it is of interest to see if the photoprotons from deuterium are produced as if the neutron and proton were independent, or if there are effects due to the proximity of the other nucleon. The relevant free nucleon reactions and the photodisintegration are:

$$\gamma + P \longrightarrow P + \pi^0$$

$$\gamma + N \longrightarrow P + \pi^-$$

$$\gamma + D \longrightarrow P + N$$

If only one deuterium nucleon interacts with the photon,

and the "spectator" nucleon does not interact with the reaction products, then the above reactions should predict the number of photoprotons from deuterium. It should be remembered that the above is not completely correct because the neutron and proton spend some fraction of the time very close together, where the spectator nucleon concept is clearly not valid. In this case it is likely that the meson would be reabsorbed by the other nucleon leading to photodisintegration or that it would scatter off the other nucleon, voiding the spectator concept. The object of the experiment is to find out to what extent the spectator model predicts the behavior of the deuteron at these energies.

II. DESCRIPTION OF THE EXPERIMENTAL METHOD

A thin walled, high pressure cylinder of hydrogen or deuterium gas cooled to liquid nitrogen temperature was bombarded with 500 mev bremsstrahlung from the Cal Tech Synchrotron. The protons emerging were observed with a telescope of three scintillation counters.

The electrons in the circulating beam of the synchrotron produced a bremsstrahlung spectrum with a 500 mev upper limit and a duration of ten milliseconds each second. The photon beam emerged from the synchrotron into the air and then passed through three collimators, the first one determining the beam size and the other two merely scraping the beam's edge. The first two collimators were holes in one foot thick lead blocks. The third collimator was four inches thick and was placed just in front of the target gas cylinder to stop any stray radiation that otherwise might strike the side of the cylinder. That the beam passed through the target without hitting the side was determined by exposing photographic film behind the target. A long exposure blackened the area that the beam hit, and a short exposure with the collimators removed would then superpose a picture of the target cylinder. When developed, the plate would show clearly the alignment of the target with respect to the beam. The beam was monitored by a Cornell type thick walled ionization chamber and the readings were corrected to standard pressure, temperature, and synchrotron energy.

The target was a stainless steel cylinder two inches in diameter and seventeen inches long, filled either with hydrogen or deuterium gas to a pressure of 2000 psi and cooled by liquid nitrogen. The temperature was measured by a thermocouple on each end of the target cylinder. These thermocouples were compared to one which was submerged in boiling nitrogen. The cooling was achieved by a collar around one end of the target which was in contact with liquid nitrogen. The observed protons did not pass through this collar.

The proton telescope is shown in figure 1. Its main components are: the tungsten slit, the absorbers A_1, A_2, and A_3, and the scintillation counters C_1, C_2, and C_3. The protons from the target were defined by 1" x 2-5/8" x 1/8" counter C_2, and the tungsten slit, 0.954 inches wide. The angular resolution function is an isosceles triangle with a base width of 4.7 degrees. The shielding of the telescope was 2" x 4" x 6" lead bricks set on end as shown to reduce the scattering of unwanted protons into the counters. The 1-1/4" x 4" x 4" lead plug in the center of the telescope was used in determining the number of protons scattered into the counters. The plug could be inserted to stop the protons which came through the slit and went directly to the counters, but permitted the counting of the protons which were scattered into the counters. Particles were required to trigger C_1 and C_2 but were rejected if they triggered C_3. Protons were separated from π mesons and electrons by the difference in specific ionization in C_1. The range to which the telescope is sensitive is from the plane in C_2 where a proton stopping will just count, to the similar

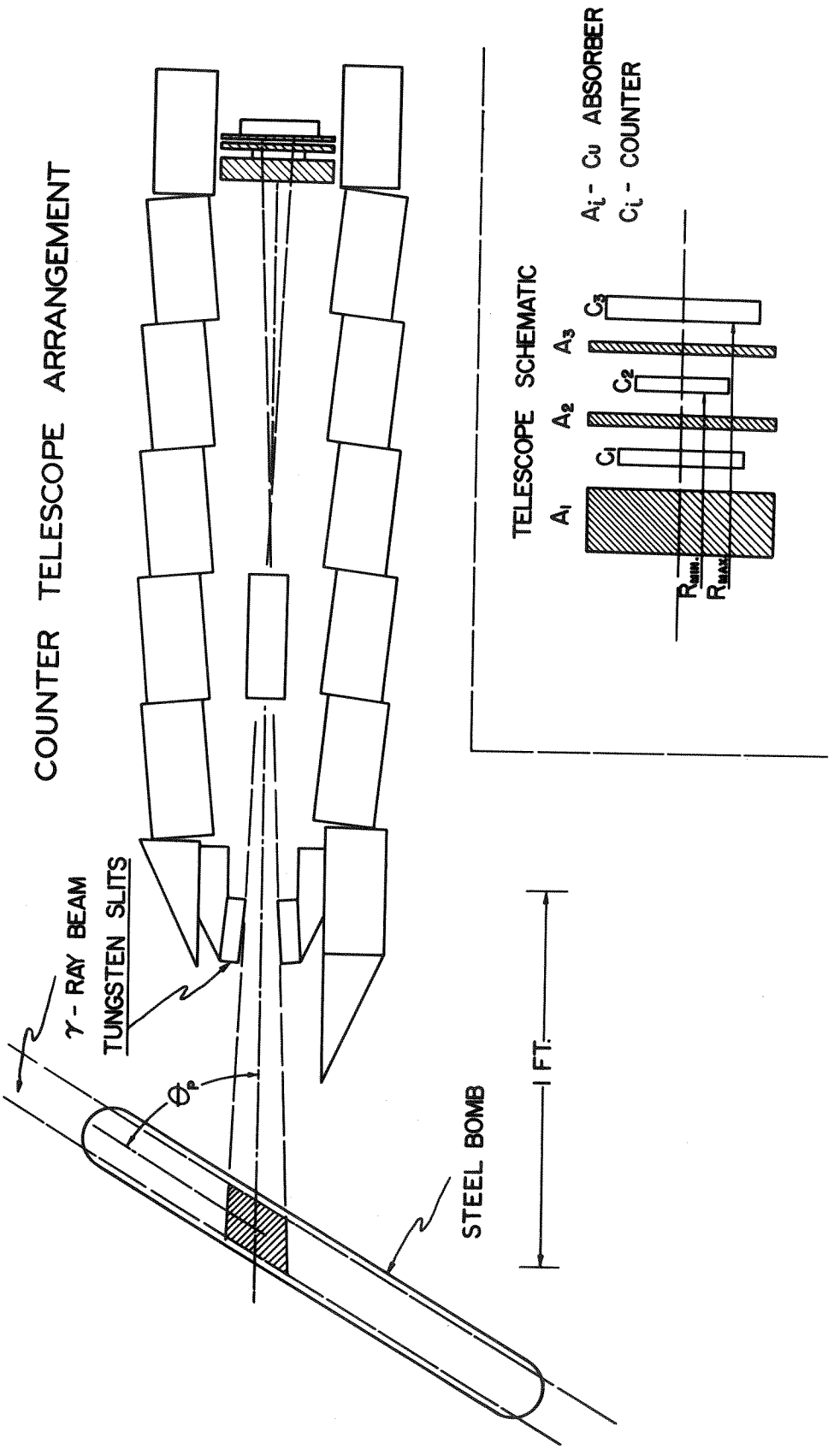
COUNTER TELESCOPE ARRANGEMENT
γ - RAY BEAM
TUNGSTEN SLITS
STEEL BOMB
1 FT.
TELESCOPE SCHEMATIC
A1 C1 A2 C2 A3 C3
Ai - Cu ABSORBER
Ci - COUNTER
RMIN.
RMAX.

FIGURE 1

plane in C_3. At higher energies ΔR was increased by putting in absorber A_3, to improve the counting rate. The proton range is the range in cm of copper of a proton which started at the center of the target and stopped in the middle of ΔR. The range was not corrected for multiple scattering as this correction is the order of 0.5%. See Bloembergen and Van Heerden (13). The range of the protons which were to be counted determined the total amount of absorber used. The absorber was divided between the three positions A_1, A_2 and A_3. The size of A_3 was determined by the energy resolution desired, taking into account the fact that counting rate increases linearly with A_3. A_2 was chosen to give the best separation of the proton and pion pulse heights in C_1. The remainder of the absorber, if any, was placed in A_1.

The output pulses from the phototubes are amplified (Synchrotron model 522 amplifiers) and fed through discriminators to the coincidence circuit. See the block diagram in figure 2. The coincidence circuit had a resolving time of 0.2 microseconds and an anticoincidence dead time of 1.3 microseconds. The desired event, coincidence between C_1 and C_2 in anticoincidence with C_3, was used to gate the twenty channel pulse height analyzer which recorded the pulse from C_1. An approximate measurement of accidental counts was made by counting the event: (C_2 triggered but C_3 not triggered) in delayed coincidence with C_1. The counting rate of the individual counters was also recorded, and was used in the analysis of the experiment to show that the above measurement of accidentals was sufficiently accurate.

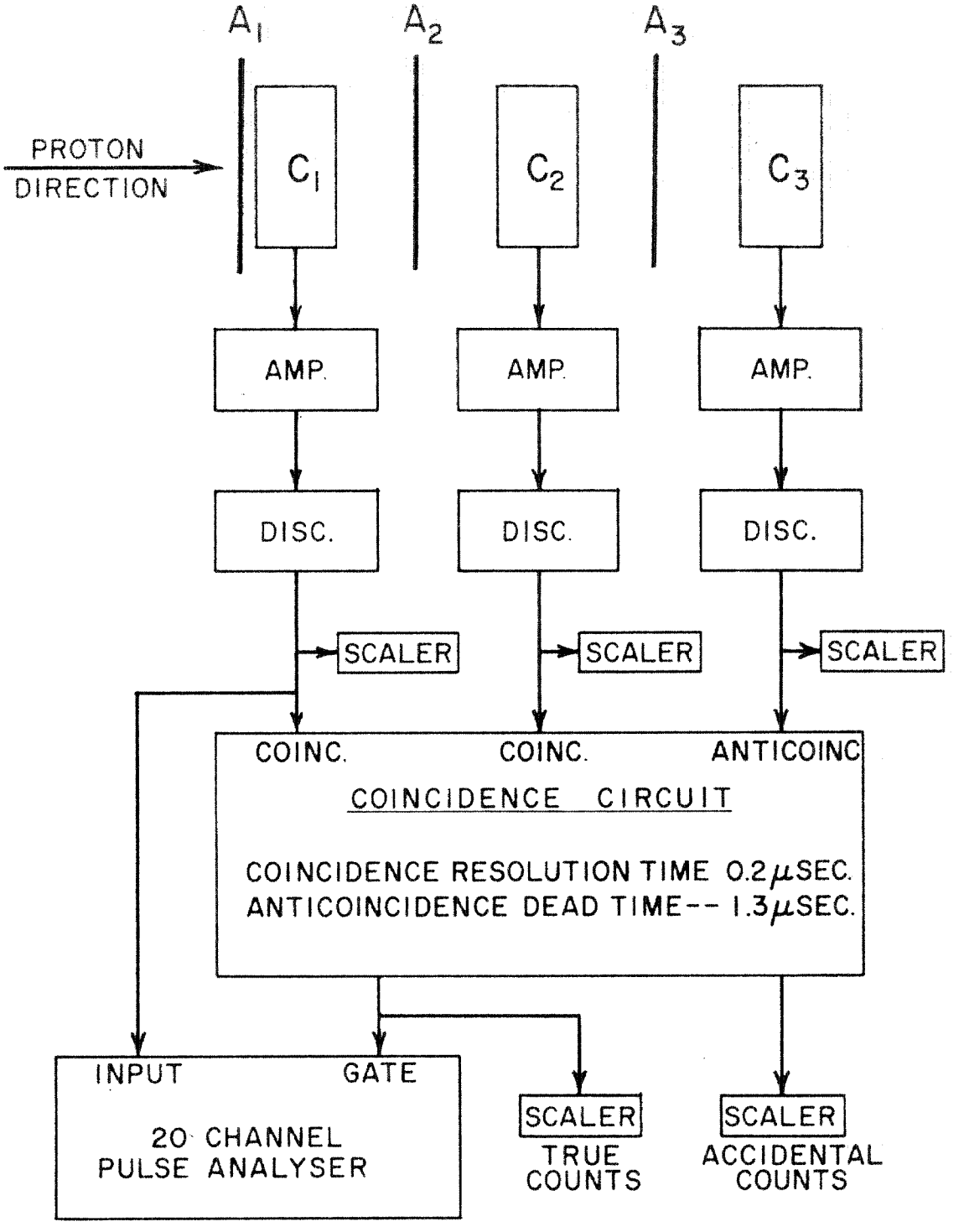

TELESCOPE ELECTRONICS

Figure 2

It is necessary to adjust the counter biases so as to discriminate against the undesired events as much as possible. However care must be taken not to affect the counting of true events. Figure 3 shows the energy lost by ionization in a scintillation counter as a function of the distance to which the particle would penetrate copper (its residual range). If the bias of a counter is set above minimum ionization then for a given particle (proton or pion), there is a region in which the particle must stop if it is to lose enough energy to exceed this bias. For a given bias this region will be much larger for protons than it will be for pions, and it is possible to set it high enough to exclude the mesons entirely; however if this were done only protons of short residual range would be counted.

The bias of C_1 was set by observing the proton and pion pulse height peaks with the twenty channel analyzer and increasing the bias of C_1 until most of the meson peak disappears. The bias of C_2 was adjusted by putting C_2 in coincidence with C_3 as a gate for the twenty channel analyzer, and using C_2 as the analyzer input. The bias on C_3 was increased to define a small ΔR. The analyzer would then show the proton peak. The bias of C_2 was then increased until the lower half of the proton peak disappeared. The largest pulses observed would come from protons which just penetrated C_3 enough to trigger it. In normal operation a proton which triggers C_3 is not counted, and C_3 is more sensitive because its bias is lower. In normal operation the proton pulses from C_2 should all be larger than the largest pulses observed from C_2 in the above calibration run, since the smaller pulses would be vetoed by C_3.

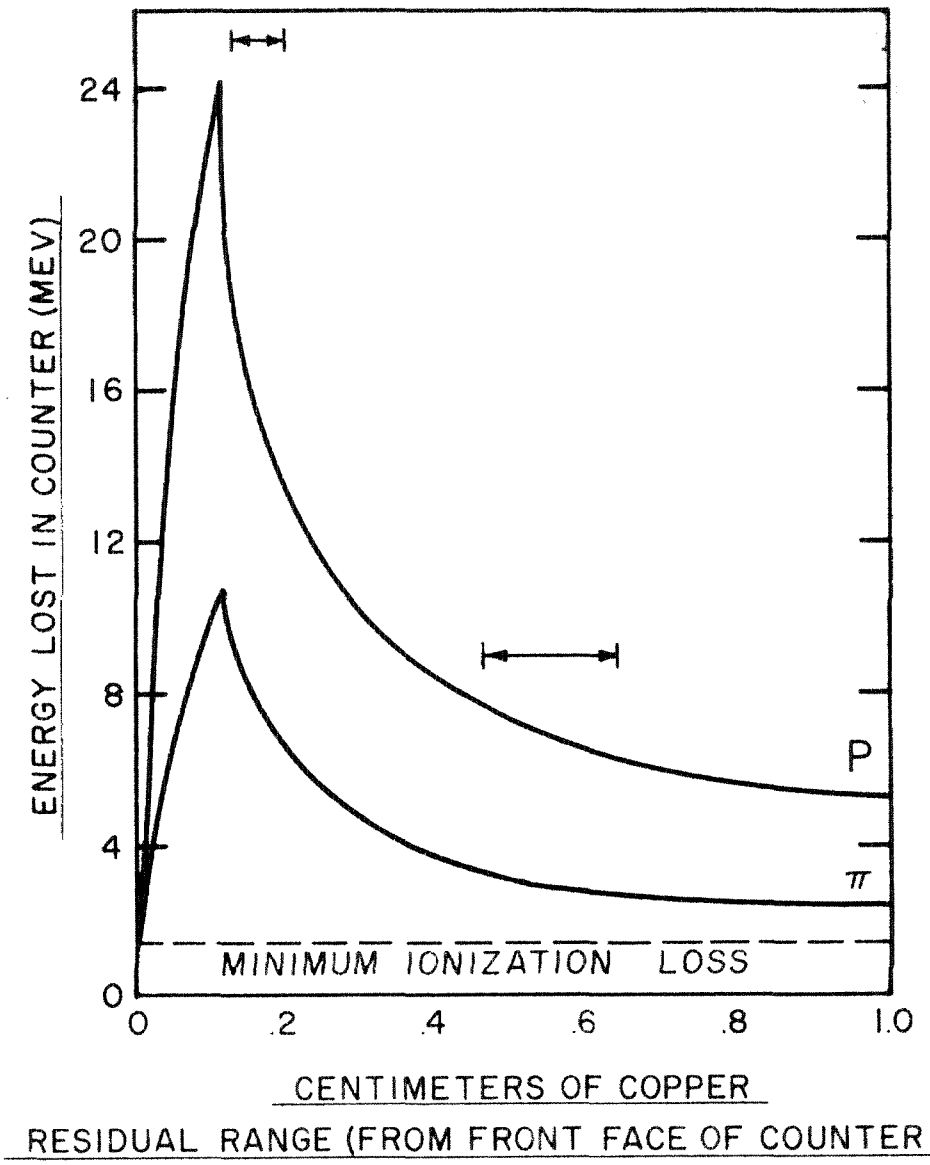

ENERGY LOST BY PROTON OR π MESON IN A 1/4" THICK PLASTIC SCINTILLATION COUNTER. THE TWO EXTREME LOCATIONS OF ΔR ARE SHOWN.

Figure 3

The above argument has assumed that the pulse height is always the same for the same energy particle. In actuality the pulse height distribution calculated from ΔR and figure 3 is smeared out by the counter resolution and was observed to be 40°/o to 100°/o wider than calculated, so setting the bias of C_2 more than 50°/o of the peak width below the peak should be safe.

The bias of C_3 was set by reducing it a factor of two from the value used while setting the bias on C_2, which gives it a margin of safety in case of electronic drift. The bias of C_3 used to set the bias of C_2 will allow C_3 to count any proton which passes through C_3 and was ionizing enough to count in C_2. Lowering the bias of C_3 reduces the required penetration of C_3 and provides a safety factor in detecting the protons which pass through C_3 and might have triggered C_2. If the bias on C_3 is reduced too far the correction for telescope deadtime may become excessive. It is not necessary for C_3 to count mesons at all, since any meson with range greater than the range for which the telescope is set will make a pulse in C_1 smaller than the meson peak, and will be excluded by the bias of C_1.

III. DETAILS OF TELESCOPE DATA REDUCTION

The telescope counting rate must be converted to a value of the laboratory cross section. The counting rate is proportional to: the photon intensity, the number of target nuclei, the solid angle subtended by the telescope, the width of the proton energy accepted by the telescope and the laboratory cross section.

Part of the target nuclei see the maximum telescope solid angle, but some of them have the solid angle reduced by the tungsten slit. The following expression for $\omega\bar{x}$, the effective product of telescope solid angle and the length of the target is derived in the appendix:

$$\omega\bar{x} = \frac{AW}{ab \sin\theta},$$

where A is the area of the smallest counter, C_2; W is the width of the tungsten slit; a is the distance from C_2 to the center of the target; b is the distance from C_2 to the tungsten slit; and θ is the angle between the photon beam and the axis of the telescope. An exact integration was carried out which agreed with this simple formula within .025 $^{o}/o$.

The width of the proton energy accepted by the telescope is determined by the quantity ΔR. The telescope counts protons with ranges in the zone $R \pm 1/2\,\Delta R$. ΔR is the range (measured in equivalent centimeters of copper) between the plane in C_2 to which a proton must penetrate to trigger it, and the similar plane in C_3. Since the counting rate is proportional to ΔR we can measure the residual ΔR (the value of ΔR when there is no absorber A_3), by

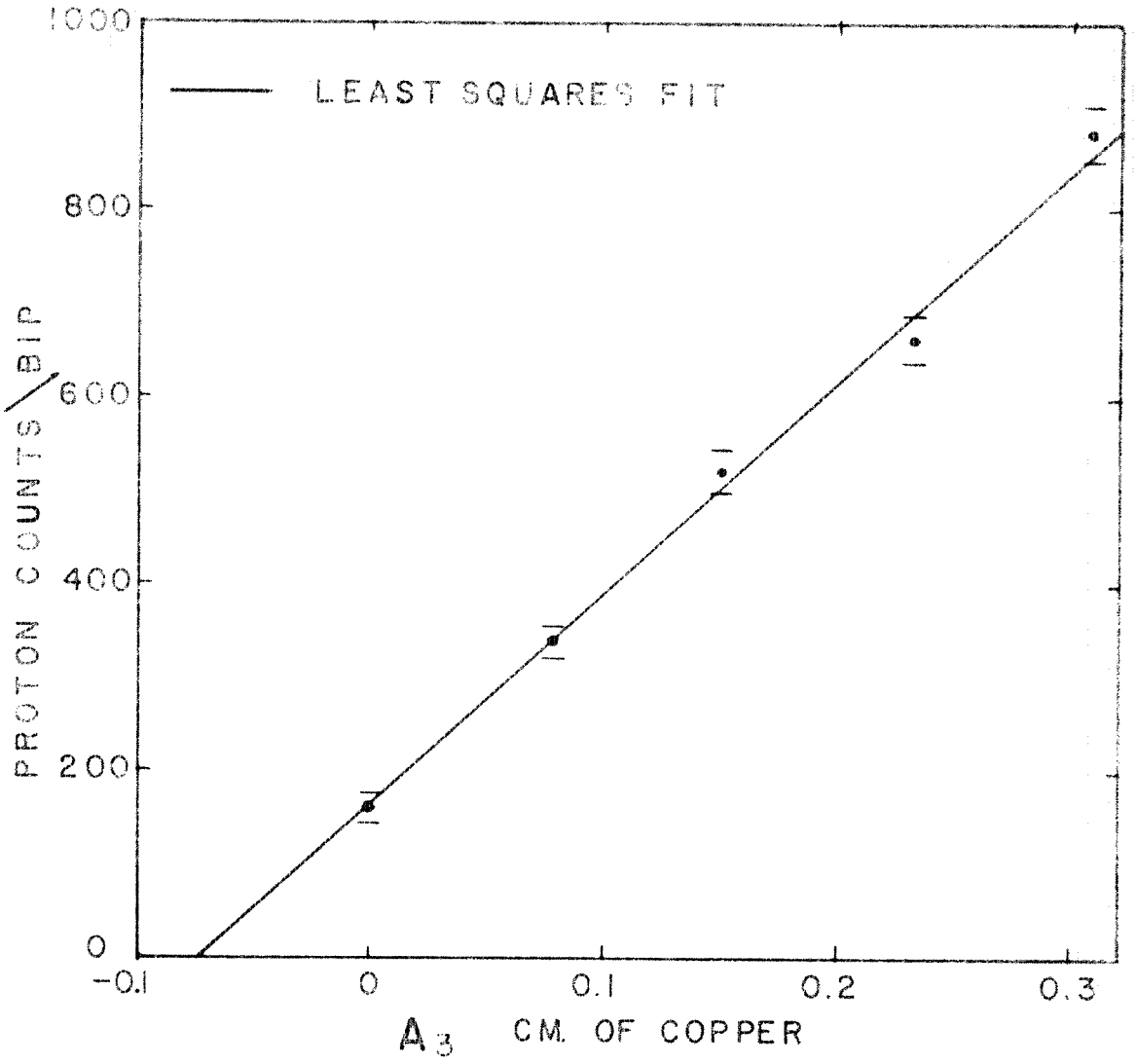

DETERMINATION OF ΔR

COUNTING RATE AS A FUNCTION OF A_3 IS EXTRAPOLATED TO ZERO COUNTS TO DETERMINE THE CONTRIBUTION TO ΔR BY COUNTERS C_2 AND C_3 THE AVERAGE OF FOUR DETERMINATIONS IS:

$$\Delta R = A_3 + .0711 \pm .0036 \text{ CM. OF COPPER}$$

Figure 4

plotting the counting rate for various values of A_3 and extrapolating to zero counts. The mean range must be kept constant by adjusting A_2 at the same time. ΔR was also calculated using range-energy tables and some approximate calculations of energy necessary to trigger counters C_2 and C_3. This result differed by 6 °/o from the average of the three determinations by the first method. The final value was obtained by averaging the four determinations with equal weight. The value obtained was $\Delta R = 0.0711 \pm 0.0036$ cm. of copper.

If the telescope were ideal $\omega \bar{x}$, R, and ΔR would be all of the information about the telescope needed to convert counting rate to proton intensity. However in actuality we must make additional corrections. Protons can penetrate the slit edges. The coincidence circuit has a finite resolution time, which allows accidental coincidences, as well as having a deadtime of 1.3 microseconds each time C_3 is triggered. The protons can be absorbed as well as slowed down by the absorbers. There is also a background counting rate which must be taken into account.

The use of 1-1/4" x 4" x 4" lead plug in the center of the telescope made possible a method of background subtraction. Data was taken with and without hydrogen and with and without the plug in position. The telescope counting rates are designated as follows: N_h = the counting rate with hydrogen in the target, N_{hp} = the counting rate with hydrogen and with the plug in position, N_v = the counting rate with the target evacuated, and N_{vp} = the counting rate with vacuum and with the plug in position. Counts originating

from sources other than the hydrogen can be divided into three classes, designated as follows: (1) counts occuring with and without the plug, (2) counts occuring only when the plug is in, (3) counts occuring only when the plug is removed. Similarly counts originating in the hydrogen can be divided into the same three classes, designated (4), (5), and (6) respectively. Now we may write:

$$N_h = (1) + (3) + (4) + (6) \qquad N_{hp} = (1) + (2) + (4) + (5)$$

$$N_v = (1) + (3) \qquad N_{vp} = (1) + (2)$$

$$N = (N_h - N_{hp}) - (N_v - N_{vp}) = (6) - (5)$$

N = *(counts from hydrogen, plug removed)* - *(counts from* hydrogen, plug in)

This method has eliminated all counts from sources other than the hydrogen. The only undesired events which could affect the counting rate are: A) untrue counts from hydrogen which are stopped when the plug is inserted, B) untrue counts from the hydrogen which are produced by the plug, (class (5)), C) true counts which somehow get through the plug and into the counter. From a study of these cases it is concluded that they are small, and further, that they tend to cancel.

Protons were lost by nuclear absorption in the target wall, in the absorbers, and in the counters. The absorption correction was calculated as a function of proton range, assuming the proton path was all in copper, using an absorption cross section which

varied with energy according to the theory of Fernbach, Serber and Taylor (2). The maximum correction was 16 °/o and a typical correction was 6 °/o.

The Fernbach, Serber and Taylor theory assumes that a particle incident on a nucleus can be represented as a wave incident on a sphere with an index of refraction and an absorption coefficient. The absorption coefficient in nuclear matter is:

$$K = \frac{3A\sigma}{4\pi R^3},$$

where R is the radius of the nucleus and σ is the cross section for scattering by the nucleons. Calculation of the absorption cross section of the nucleus gives:

$$\sigma_a = \pi R^2 \left\{ 1 - \left[1 - (1 + 2KR) e^{-2KR} \right] \frac{1}{2K^2 R^2} \right\}.$$

To calculate K we use a weighted average of the np and pp cross sections:

$$\sigma = \frac{1}{A} \left[Z\,\sigma_{pp} + (A-Z)\,\sigma_{np} \right].$$

The pp and np cross sections in nuclear matter are smaller than the corresponding cross sections for free nucleons because the exclusion principle forbids the interaction in cases where the scattered nucleons would have energy less than the Fermi energy, since all of the states are filled below the Fermi energy.

This reduction has been calculated by Goldberger. (16)

$$\sigma = \left(1 - \frac{7}{5P_o^2}\right) \sigma_{free} = \left(1 - \frac{1.4\, E_f}{E + V}\right) \sigma_{free},$$

where

Po = Momentum of particle inside of the nucleus relative to Fermi momentum;

E_f = Fermi energy;

E = Energy of the particle outside of the well;

V = Nuclear well depth.

We now have:

$$\sigma = \left(1 - \frac{35}{E + 30}\right) \frac{1}{A} \left\{ Z\, \sigma_{pp} + (A - Z)\, \sigma_{np} \right\},$$

where the free nucleon cross sections are now used. E_f = 25 mev, V = 30 mev and E is the energy of the incident proton outside of the nucleus in mev. Using the np and pp cross sections quoted by (17) Rossi the absorption cross section of copper as a function of energy was calculated. This was then integrated to obtain the function F(r) which is the fraction of the protons of range r that come to rest in copper without being absorbed. Since the absorption of a proton after it has triggered C_2 is permissible, the corrected counting rate is the measured counting rate multiplied by the factor:

$$\frac{F(\frac{1}{2}\Delta r)}{F(r)}.$$

Counts contributed by higher energy protons which stopped in ΔR due to nuclear absorption were calculated using the known proton

spectrum. This effect should be most important at the lowest energy at 29.7°; in this case the correction was calculated to be 1.5 °/o and was neglected.

The accidental channel recorded the accidentals only approximately. An analysis showed that the approximation was as good as was required, since the accidental correction was never more than 8 °/o. An accidental spectrum was taken by feeding the pulses from C_1 into the pulse height analyzer without requiring a gate. This showed the fraction of the accidental counts which actually counted in the proton peak channels.

The tungsten slits were set at an angle such that it was impossible for a proton scattered off the slit face to reach the counters. A calculation of the correction for slit edge penetration, neglecting scattering, was made using the known proton spectrum and the requirement that after penetrating the slit edge the proton must have the proper energy to count in the telescope. This correction was 4 °/o at most and was typically 2 °/o. The correction was adjusted to account for scattering in the following way. An average mean square scattering angle was calculated for protons penetrating the slit edge. This was done by dividing the slit edge into zones and finding the number of protons (in the proper energy interval) and their mean square scattering angle from each zone, for a given angle of incidence on the slit. A weighted mean square scattering angle was then obtained by combining the zones. This was then integrated over the target and the incident angle. This result was used to correct the preceding

calculation of penetration without scattering. This calculation showed that at most the simpler penetration calculation was 26 °/o too small.

Some pulses were observed from C_1 which were larger than the usual proton pulses, and could not be reasonably explained as accidentals, the number of which could be estimated. An estimate of star production in C_1 showed that the number of these large pulses was of the right order of magnitude to be accounted for by multiple prong stars. This suggested that there were single prong stars which were being counted as protons. From Lees, et al (3) it was ascertained that the ratio of multi prong stars to single prong stars was 3 ± 1 for heavy nuclei. Assuming this figure applies, the correction for single prong stars is less than 0.8 °/o in all cases.

There is a possibility that the recoil deuterons from the reaction $\gamma + D \longrightarrow D + \pi^o$ might have contributed large pulses in the deuterium runs. This reaction has been investigated in the photon energy region 250 to 300 mev by Wolfe, Silverman and De Wire (19) at Cornell and Rosengren and Baron (20) at M.I.T. Upon examining the dynamics of the reaction it was found kinematically impossible for deuterons to contribute to the counting rate, except at the four lowest energy points at 29.7^o and the two lowest energy points at 41.2^o. Since the probability of the deuteron remaining bound falls off rapidly with increasing recoil momentum, we will estimate the number of deuterons counted at the lowest energy point at 29.7^o, which requires a photon energy

of 380 mev.

From Wolfe, Silverman and De Wire we may write the elastic pion cross section from deuterium as:

$$\sigma = |A_N + A_P|^2 \left[\int \psi_0(r)^2 \exp(\tfrac{1}{2} i \mathbb{D} \cdot \mathbb{r}) \, d\mathbb{r}\right]^2,$$

where: A_n is the amplitude for neutral pion production from the neutron;

A_p is the amplitude for neutral pion production from the proton;

$\psi_0(r)$ is the deuteron ground state wave function;

D is the impulse given to the deuteron in the production of the meson.

To estimate the cross section at higher energy we assume that A_n is proportional to A_p and that the phase difference between them is constant, giving:

$$\sigma \propto |A_P|^2 \left[F(D)\right]^2,$$

or, since the cross section is proportional to the square of the amplitude:

$$\sigma \propto \sigma_{\pi^0_H} \left[F(D)\right]^2,$$

where:

$$F(D) = \int \psi_0(r)^2 \exp(\tfrac{1}{2} i \mathbb{D} \cdot \mathbb{r}) \, d\mathbb{r}.$$

The measured value of the elastic pion cross section of deuterium at a meson angle of 110^{o} in the laboratory is 2.5 microbarns per steradian (lab). We transform this to the center of mass system, extrapolate it to higher energy, and transform it to the lab system of the deuteron obtaining 0.16 microbarns per steradian. A factor of 1/5 was introduced by $[F(D)]^2$, the change in the pion cross section from hydrogen introduced a factor of 2/3, and the rest of the change was from the two solid angle transformations. This cross section will produce a counting rate of .005 counts/bip. At the low energy setting at 29.7^{o} the deuterium counting rate was 3.1 counts/bip so the deuterons would contribute only 1/600 of the counts, and these would probably have been discarded by their pulse height.

IV. INTERPRETATION OF THE DEUTERIUM DATA

The observed photo protons from deuterium can be attributed to three reactions:

$$\gamma + D = P + N,$$
$$\gamma + D = \pi^{o} + P + N,$$
$$\gamma + D = \pi^{-} + P + P.$$

The second and third of the above reactions are three body reactions, where we can not completely determine the reaction by observing only one particle. Since the deuteron is relatively loosely bound (2.23 mev) and the average nucleon spacing is moderately large, it is worth while to see if the data is consistent with the assumption that the photon interacts with only one of the two nucleons, leaving the other as a spectator. This is an important assumption upon which all of the following work is based. It should be kept in mind that all of the recoil protons observed had an energy of 46 mev or more, which corresponds to a momentum of 300 mev/c, while the median momentum of the nucleons in deuterium is around 50 mev/c. If we allow the above assumption we may rewrite the reactions as follows:

$$\gamma + D = P + N,$$
$$\gamma + P_{D} = P + \pi^{o},$$
$$\gamma + N_{D} = P + \pi^{-},$$

where the subscript D indicates that the target nucleons are moving with the momentum distribution which they have in deuterium.

The reactions are now to be regarded as two body reactions. For a given recoil proton energy the incident photon energy is much lower for the photodisintegration reaction than for the meson producing reactions. This property allows the photo disintegration cross section to be measured separately by lowering the energy of the bremsstrahlung spectrum. This experiment has been carried out by Keck and Tollestrup (10) of this laboratory. From their results it is possible to calculate the number of counts produced by that reaction and to subtract them, leaving only the counts due to the meson producing reactions.

This correction was made using the angular distribution coefficients shown in figure 5. Over the region where it was possible the data of Keck and Tollestrup (10) (Cal Tech) was used. The curves were extended downward to a photon energy of 80 mev using the data of Whalin, Schriever and Hanson (11) (University of Illinois). The Illinois data was in the form of angular distribution coefficients for the expression $(A + B\sin^2\theta)(1 + 2\beta\cos\theta)$ which when expanded gives: $(A + B) + 2\beta(A + B)\cos\theta - B\cos^2\theta - 2\beta B\cos^3\theta$. This can not be directly compared with the A, B, and C coefficients of the Keck and Tollestrup expansion $A + B\cos\theta + C\cos^2\theta$, which contains only one term asymmetrical about 90 degrees. In order to compare the data it was assumed that $2B\beta\cos^3\theta = B\beta\cos\theta$. This change did not make any important change in the angular distribution curve and allowed the use of the Illinois data to extrapolate the coefficients of Keck and Tollestrup to 80 mev. The Cal Tech coefficients together with the coefficients obtained from the Illinois data and the Cornell coefficients quoted by Keck and Tollestrup are shown in

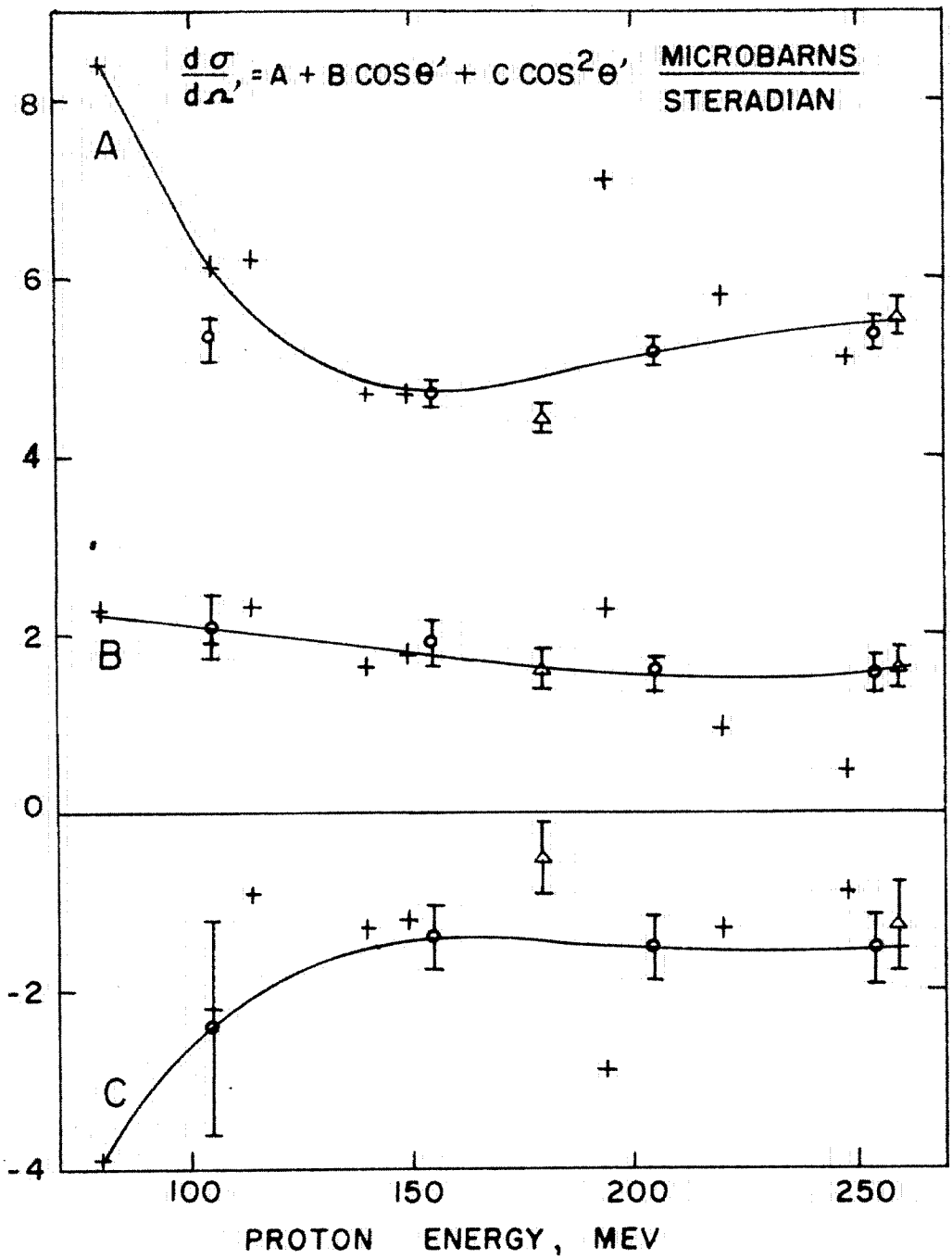

DEUTERIUM PHOTODISINTEGRATION ANGULAR DISTRIBUTION COEFFICIENTS.

CALTECH CORNELL + ILLINOIS

CURVES SHOW VALUES USED FOR DATA CORRECTION

Figure 5

figure 5. In drawing the curves to be used in this experiment the Cal Tech data was given the most weight because of the fact that this experiment used the same synchrotron beam monitoring equipment, deuterium target and density measuring equipment, and a similar type of proton telescope. By using their data possible absolute calibration errors are avoided. In addition it is pointed out that the Illinois data is mostly consistent with the Cal Tech data. From these coefficients the number of photodisintegration protons was calculated, corrected for absorption, and subtracted for each setting of the telescope. The fraction of the deuterium photoprotons from photodisintegration for each of the three telescope angles is, 29.7 degrees: 11°/o to 20°/o except for the highest energy point which was 25°/o, 41.2 degrees: 16°/o to 23°/o, 51.8 degrees: 32°/o to 39°/o.

The cross section for the reaction $\gamma + P = P + \pi^o$ is known, both from the first portion of this experiment and from the experiments of others. The cross section for the reaction $\gamma + N = P + \pi^-$ is somewhat less accurately known, but can be inferred from the experiment of Sands, Teasdale and Walker (6). From these cross sections and a knowledge of the momentum of the nucleons in the deuteron it is possible to calculate the corrected counting rate that should have been observed. In order to reduce errors caused by the absolute calibration of the telescope and the beam monitoring equipment, ratios of counting rates of deuterium and hydrogen, corrected for photo disintegration were calculated.

V. DEUTERIUM DYNAMICS CALCULATION

In the case of a proton telescope looking at a hydrogen target bombarded by photons, the counting rate is proportional to the appropriate differential cross section. If the target nucleons are moving, as in deuterium, then the counting rate is no longer dependent only on one particular value of the cross section, but it depends on a weighted average of the cross section over neighboring energies and angles. The problem now is to find this weighting function. It was decided to do this by considering two hundred equally probable initial momenta for the target nucleon. For each momentum the following quantities were calculated, using the condition that the recoil proton be counted by the telescope. The laboratory energy of the incident photon K, the apparent photon energy as seen by the target nucleon K_o, the center of mass angle between the incident photon and the recoil proton δ, and a weighting function which will be described later. The quantities K_o and $\cos\delta$ determine the point where the differential cross section is sampled (the dots in figures 6 and 7). Single meson production cross section can be described as a function of two variables, for example: $\frac{d\sigma}{d\Omega'} = \frac{d\sigma}{d\Omega'}(K_o, \cos\delta)$, where K_o is the photon energy as observed from the target nucleon and δ is the angle between the photon and the recoil proton in the center of mass system (in general, primes denote center of mass system). A contour map of cross section can be made as shown in figures 6, 7 and 8. If our telescope is set to observe the cross section at some point when the target nucleon is at rest, then as the nucleon assumes each of the two hundred values of momentum we

CONTOUR MAP OF DIFFERENTIAL CROSS SECTION
FOR THE REACTIONS $\gamma + P \rightarrow P + \pi^{\circ}$ $\gamma + N \rightarrow P + \pi^{-}$
UNITS ARE μ BARNS/STERADIAN

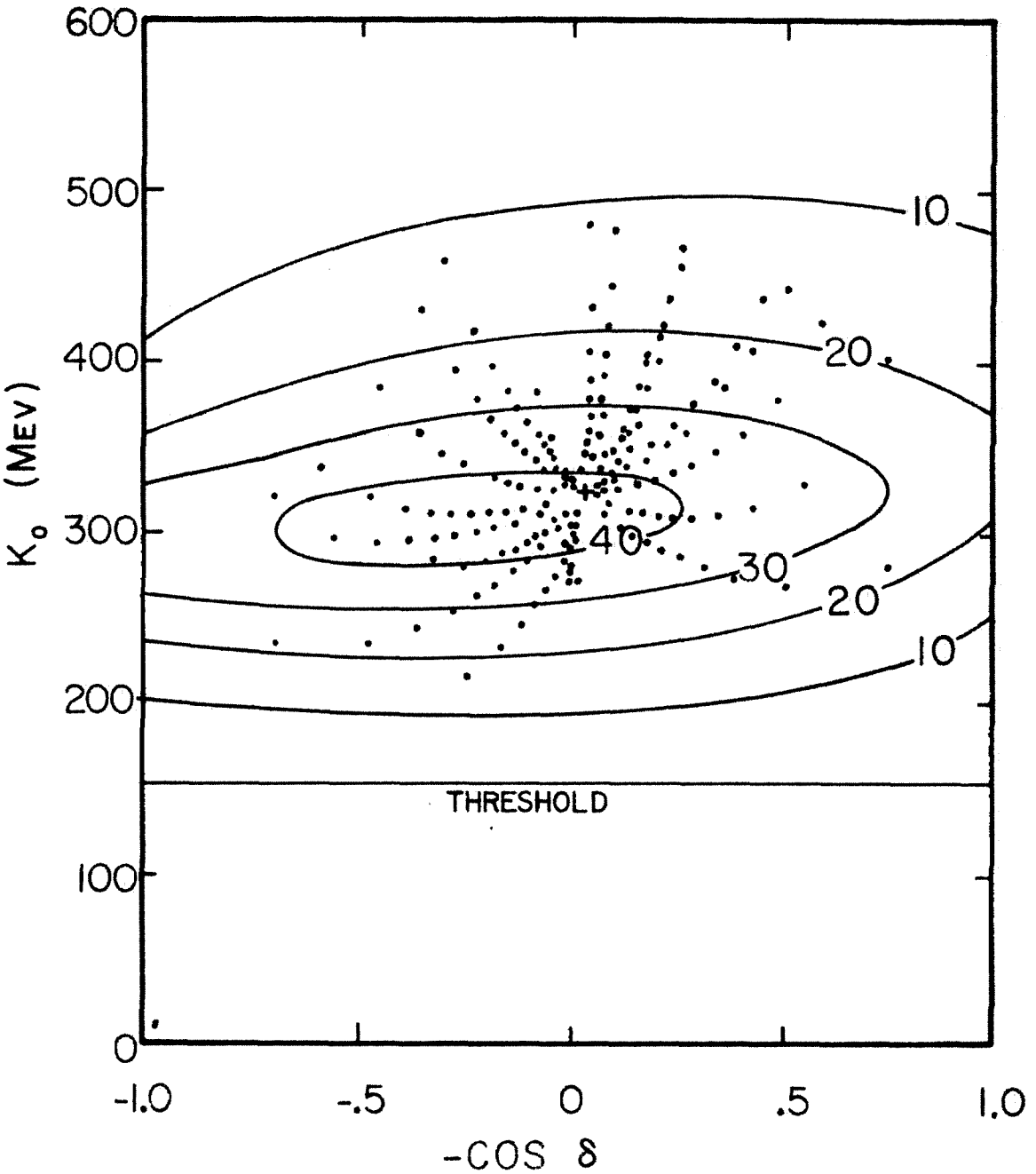

THE POINTS SHOW THE SMEARING EFFECT OF DEUTERIUM WHEN RECOIL PROTONS ARE OBSERVED.

Figure 6

CONTOUR MAP OF DIFFERENTIAL CROSS SECTION FOR THE REACTIONS $\gamma + P \rightarrow P + \pi^0$ $\gamma + N \rightarrow P + \pi^-$ UNITS ARE μ BARNS / STERADIAN

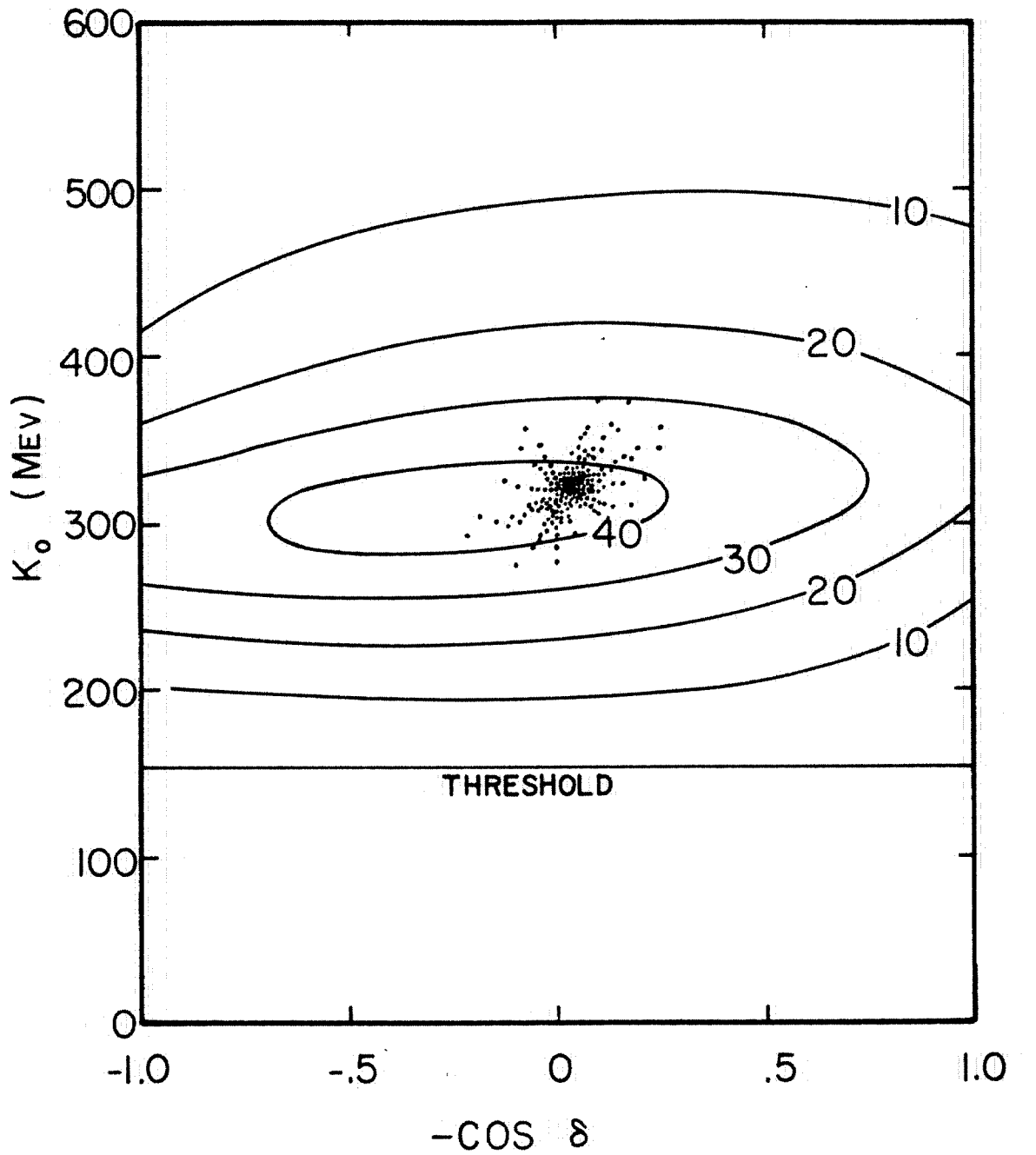

THE POINTS SHOW THE SMEARING EFFECT OF DEUTERIUM WHEN THE MESONS ARE OBSERVED

Figure 7

CONTOUR MAP OF DIFFERENTIAL CROSS SECTION FOR THE REACTIONS $\gamma + P \rightarrow P + \pi^{\circ}$ $\gamma + N \rightarrow P + \pi^{-}$ UNITS ARE μ BARNS/STERADIAN

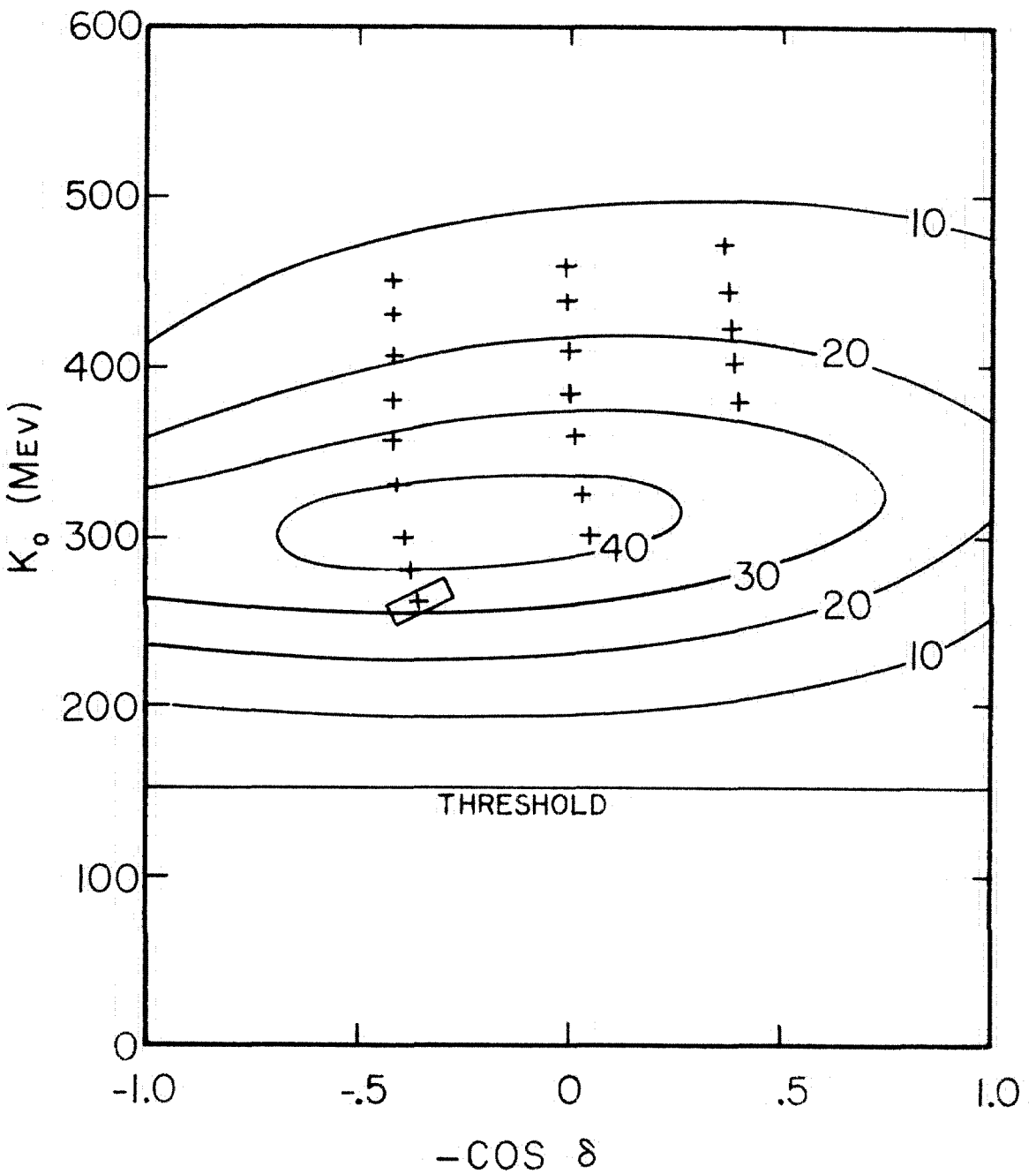

POSITIONS AT WHICH DATA WAS TAKEN WITH THE PROTON TELESCOPE. THE PARALLELOGRAM SHOWS THE TELESCOPE APERTURE.

Figure 8

sample the cross section at each of the points shown. There are less than two hundred points shown because for some momenta it is impossible to produce the required recoil with a photon of 500 mev or less. The two hundred momenta were chosen to represent the motion of the nucleons in deuterium as follows. Twenty spherically symmetric directions were chosen. These are the perpendiculars to the faces of a regular icosahedron. Ten values of momentum were chosen to represent the momentum spectrum. They were selected so that there was a 5% probability of a nucleon with momentum less than the first value, 15% for the second value, and so on up to 95% probability of a nucleon with momentum less than the tenth value. Two deuteron wave functions were tried and both gave practically the same ten values of momentum. One was the familiar Hulthen wave function and the other was the Gartenhaus (7) wave function, derived from the cut-off Yukawa meson theory.

To find the weighting function let us first consider the calculation of the contribution to the counting rate of one particular nucleon momentum:

$$\text{number of counts} = \iint N \frac{d\sigma}{d\Omega'} d\Omega' \frac{dn}{dK_o} dK_o ,$$

where the integral is carried out over the aperture of the telescope in K_o, Ω' space, And where: N = the number of target nucleons/cm^2 with the particular value of initial momentum; $N \frac{d\sigma}{d\Omega'}$ = the probability per unit solid angle of a photon of energy K_o producing a meson at an angle $\pi - \delta$ in the center of mass system; $\Delta K_o (\frac{dn}{dK_o})$ = the number of photons in the energy range $K_o \pm 1/2 \Delta K_o$. If the

aperture of the telescope is sufficiently small, as it was designed to be, then we may replace the integrand by its value at the center of the aperture and take it outside of the integral, obtaining:

$$\text{counts} = N\frac{d\sigma}{d\Omega'}\frac{dn}{dK_o}\iint dK_o d\Omega', \text{ where: } K_o = \frac{1-\beta_n \cos\theta_n}{\sqrt{1-\beta_n^2}} K ;$$

β_n is the target nucleon velocity; θ_n is the angle between photon and nucleon.

Since K_o and K are related by a constant the integral is immediately transformed to K, Ω' space:

$$\text{counts} = N\frac{d\sigma}{d\Omega'}\frac{dn}{dK_o}\frac{1-\beta_n\cos\theta_n}{\sqrt{1-\beta_n^2}}\iint dK\, d\Omega' = A\iint dK\, d\Omega' ,$$

and:

$$\int d\Omega' = \iint \sin\alpha' d\gamma' d\alpha' = \iint d\gamma' d(\cos\alpha') ,$$

where: α', γ' is a spherical coordinate system with its axis parallel to the velocity of the center of mass with respect to the laboratory, α' is the polar angle and γ' is the azimuthal angle. The transformation from this system to the laboratory system α, γ is found by considering a particle moving in the α', γ' direction with a velocity β' (relative to the speed of light). It is shown later that the transformation equations are:

$$\cos\alpha = \frac{\beta_{cm} + \beta'\cos\alpha'}{\sqrt{\beta_{cm}^2 + \beta'^2 + 2\beta_{cm}\beta'\cos\alpha' - \beta'^2\beta_{cm}^2(1-\cos^2\alpha')}} , \quad \gamma = \gamma' .$$

where β_{cm} is the velocity of the center of mass relative to the laboratory. We may now write:

$$\text{counts} = A\iint dK \left.\frac{\partial(\cos\alpha')}{\partial(\cos\alpha)}\right|_K d\Omega ,$$

since: $$\int d\Omega' = \iint d\gamma' d(\cos\alpha') = \iint d\gamma \left.\frac{\partial(\cos\alpha')}{\partial(\cos\alpha)}\right|_K d(\cos\alpha) = \int \left.\frac{\partial(\cos\alpha')}{\partial(\cos\alpha)}\right|_K d\Omega .$$

Now writing $d\Omega = d\phi_p d(\cos\theta_p)$, we obtain

$$\text{counts} = A\iiint dK \left.\frac{\partial(\cos\alpha')}{\partial(\cos\alpha)}\right|_K d\phi_p d(\cos\theta_p).$$

We wish to further transform this integral from K, $\cos\theta_p$ space to T_p, $\cos\theta_p$ space:

$$\text{counts} = A\iiint \left.\frac{\partial K}{\partial T_p}\right|_{\theta_p} \left.\frac{\partial(\cos\alpha')}{\partial(\cos\alpha)}\right|_K d\phi_p d(\cos\theta_p) dT_p .$$

Again since our aperture has been taken small we will evaluate the partial derivatives at the center of the aperture and take them outside of the integral:

$$\text{counts} = A \left.\frac{\partial K}{\partial T_p}\right|_{\theta_p} \left.\frac{\partial\cos\alpha'}{\partial\cos\alpha}\right|_K \iint dT_p d\Omega = A \left.\frac{\partial K}{\partial T_p}\right|_{\theta_p} \left.\frac{\partial\cos\alpha'}{\partial\cos\alpha}\right|_K \Delta T_p \Delta\Omega ,$$

$$\text{counts} = N \frac{d\sigma}{d\Omega'} \frac{d\eta}{dK_0} \frac{1-\beta_n\cos\theta_n}{\sqrt{1-\beta_n^2}} \left.\frac{\partial K}{\partial T_p}\right|_{\theta_p} \left.\frac{\partial\cos\alpha'}{\partial\cos\alpha}\right|_K \Delta T_p \Delta\Omega ,$$

where ΔT_p is the proton energy acceptance of the telescope and $\Delta\Omega$ is the solid angle subtended by the telescope at the target.

Consider a nucleon gas confined to the region $0 \leq X \leq a$ bombarded by photons traveling in the positive X direction. The nucleons are equally distributed among the two hundred states

which we have chosen for the problem. Each state is defined by a set of values of β_n, θ_n, ϕ_n, where the axis of the polar coordinate system is chosen to be the X axis. If $\cos\theta_n$ is positive then a nucleon in that state will appear at the X = O boundary, move to the right with the velocity $\beta_n C \cos\theta_n$, and disappear at the X = a boundary. While a photon is traversing the target in a time $\frac{a}{C}$ a fraction of the nucleons $\frac{\frac{a}{c}\beta_n C \cos\theta_n}{a} = \beta_n \cos\theta_n$ will have disappeared at the X = a boundary, and a like number will have appeared at the X = O boundary. The photon will have opportunity to collide with only $N_e = (1-\beta_n \cos\theta_n)N$ of the N target nucleons in that state. N_e will be called the effective number of nucleons in that state. It is seen that this expression is also valid for $\cos\theta_n$ less than zero. It is now clear that N should be replaced by N_e in the preceding counting rate equation, giving:

$$\text{counts} = N \frac{d\sigma}{d\Omega'} \frac{dn}{dK_o} \frac{(1-\beta_n \cos\theta_n)^2}{\sqrt{1-\beta_n^2}} \left.\frac{\partial K}{\partial T_p}\right|_{\theta_p} \left.\frac{\partial \cos\alpha'}{\partial \cos\alpha}\right|_K \Delta T_p \, \Delta\Omega .$$

We now obtain an expression for the incident photon spectrum. The synchrotron photon spectrum can be described by:

$$\frac{dn}{dK} = \frac{f(K)}{KE_o} G ,$$

where G is the total energy in the photon beam, K is the photon energy of interest and f(K) is the bremsstrahlung energy distribution function which depends on the electron energy E_o and on the target material. f(K) has the property that:

$\int_0^{E_o} f(K)dK = 1$. $G \times \frac{\Delta K}{E_o} \times f(K)$ = the energy in the interval $K \pm \frac{1}{2}\Delta K$.

$\frac{dn}{dK} \Delta K = G\frac{f(K)}{KE_o} \Delta K$ = the number of photons in the interval $K \pm \frac{1}{2}\Delta K$.

Similarly:

$\frac{dn}{dK_o} \Delta K_o$ = the number of photons in the interval $K_o \pm \frac{1}{2}\Delta K_o$.

Since the number of photons in ΔK_o must equal the number in the corresponding region ΔK in the K spectrum, and:

$$K_o = \frac{1-\beta_n \cos\theta_n}{\sqrt{1-\beta_n^2}} K ,$$

we have:

$$\frac{dn}{dK_o} \Delta K_o = \frac{dn}{dK_o} \frac{1-\beta_n \cos\theta_n}{\sqrt{1-\beta_n^2}} \Delta K = \frac{dn}{dK} \Delta K ,$$

and:

$$\frac{dn}{dK_o} = \frac{\sqrt{1-\beta_n^2}}{1-\beta_n \cos\theta_n} \frac{dn}{dK} = \frac{\sqrt{1-\beta_n^2}}{1-\beta_n \cos\theta_n} \frac{f(K)}{KE_o} G .$$

Substituting this into the equation for counts we obtain:

$$\text{counts} = GN \left\{ \frac{f(K)}{KE_o} \frac{\partial K}{\partial T_p}\bigg|_{\theta_p} \frac{\partial \cos\alpha'}{\partial \cos\alpha}\bigg|_K (1-\beta_n \cos\theta_n) \right\} \frac{d\sigma}{d\Omega'} \Delta T_p \Delta\Omega .$$

The expression inside the brackets will be referred to as the weighting function. We may now write the expression for the total counts from all of the two hundred possible initial momenta of the target nucleon:

$$\text{total counts} = \Delta T_p \, \Delta\Omega \, G \, \frac{N_o}{200} \sum_{1}^{200} \left\{ \frac{f(K)}{K E_o} \frac{\partial K}{\partial T_p}\bigg|_{\theta_p} \frac{\partial \cos\alpha'}{\partial \cos\alpha}\bigg|_{K} (1 - \beta_n \cos\theta_n) \right\} \frac{d\sigma}{d\Omega'} .$$

Where N has been replaced by $N_o/200$, N_o being the total number of target nucleons. It is now seen that each value of $\frac{d\sigma}{d\Omega'}$, determined by K_o, and $\cos\delta$ is weighted by the expression inside of the brackets. More details of this calculation and the Datatron digital computer program used to carry it out are described in the appendix.

VI. RESULTS OF THE π^o CROSS SECTION MEASUREMENT

The photoprotons from hydrogen can come from three reactions:

$$\gamma + P = P + \pi^o, \qquad \gamma + P = P + \gamma', \qquad \gamma + P = P + \pi + \pi.$$

The second of these is the compton scattering of photons from protons. This reaction has been looked for by Ernstene, Tollestrup and Keck (4), who stated that the cross section is less than 2 $^o/o$ of the π^o cross section.

The pair production reaction can conceivably contribute recoil protons for some of the telescope settings. To find the telescope settings for which it is kinematically impossible to observe proton recoils from π pair production, the extreme case was examined where the two π mesons go together and give the proton the greatest possible recoil. In this way it was shown to be impossible for the π pair recoils to contribute to the counting rate of the thirteen telescope settings which corresponded to a photon energy greater than 360 mev for π^o production. Cutkosky and Zachariasen (5) have investigated π pair production theoretically and state that the most probable mode of pair production at low energy is with the π^+ meson in a p state and the π^- in an s state. Generally speaking the π^+ will have more energy than the π^-, hence the extreme case where the mesons go together is not very probable. It seems reasonable that there is a region below the absolutely safe region in which one is moderately safe in assuming that π pair production does not contribute energetic proton recoils.

An experimental check was made at the lowest energy at the 41.2 degree telescope setting by lowering the synchrotron energy to 408 mev for one run. The cross section obtained from this run was (9 ± 6) °/o larger than the value obtained at 500 mev, which is a discrepancy in the opposite direction from the possible effect of pair production. Since the second two of the above reactions make negligible contributions to the photoproton spectrum, the photoprotons must come from the first reaction. We can calculate the π^o meson production cross section from the photoproton spectrum.

The probability that a photon passing through the target will produce a recoil proton which counts in the telescope is: $\frac{d\sigma}{d\Omega} A \omega \bar{x} \rho$. Where: $\frac{d\sigma}{d\Omega}$ is the laboratory cross section in cm^2/steradian, A is Avogadro's number (hydrogen atoms/gram), $\omega \bar{x}$ is the effective product of the solid angle subtended by the telescope and the length of the target, ρ is the density of hydrogen in grams/cm^3. The number of photons per bip (beam integrator pulse) in the energy interval $K + 1/2\Delta K$ is $\frac{f(K)\Delta K}{KE} G$. Where: f(K) is the bremsstrahlung function, E is the synchrotron energy, and G is the total beam energy per bip ($G = 1.00 \times 10^{12}$ mev/bip)*. The counting rate in counts per bip is: $N/bip = \frac{d\sigma}{d\Omega} A \omega \bar{x} \rho \frac{f(K)\Delta K}{KE} G$. ΔK is related to ΔR by the relation: $\Delta K = \frac{\partial K}{\partial T_p}\Big|_{\cos\theta} \frac{dT_p}{dR} \Delta R$. $\frac{dT_p}{dR}$ is the rate at which energy is lost by a proton passing

---

* This value is an average of a determination by the shower method (21) and a determination with a pair spectrometer (22). The 15 °/o discrepancy is unresolved.

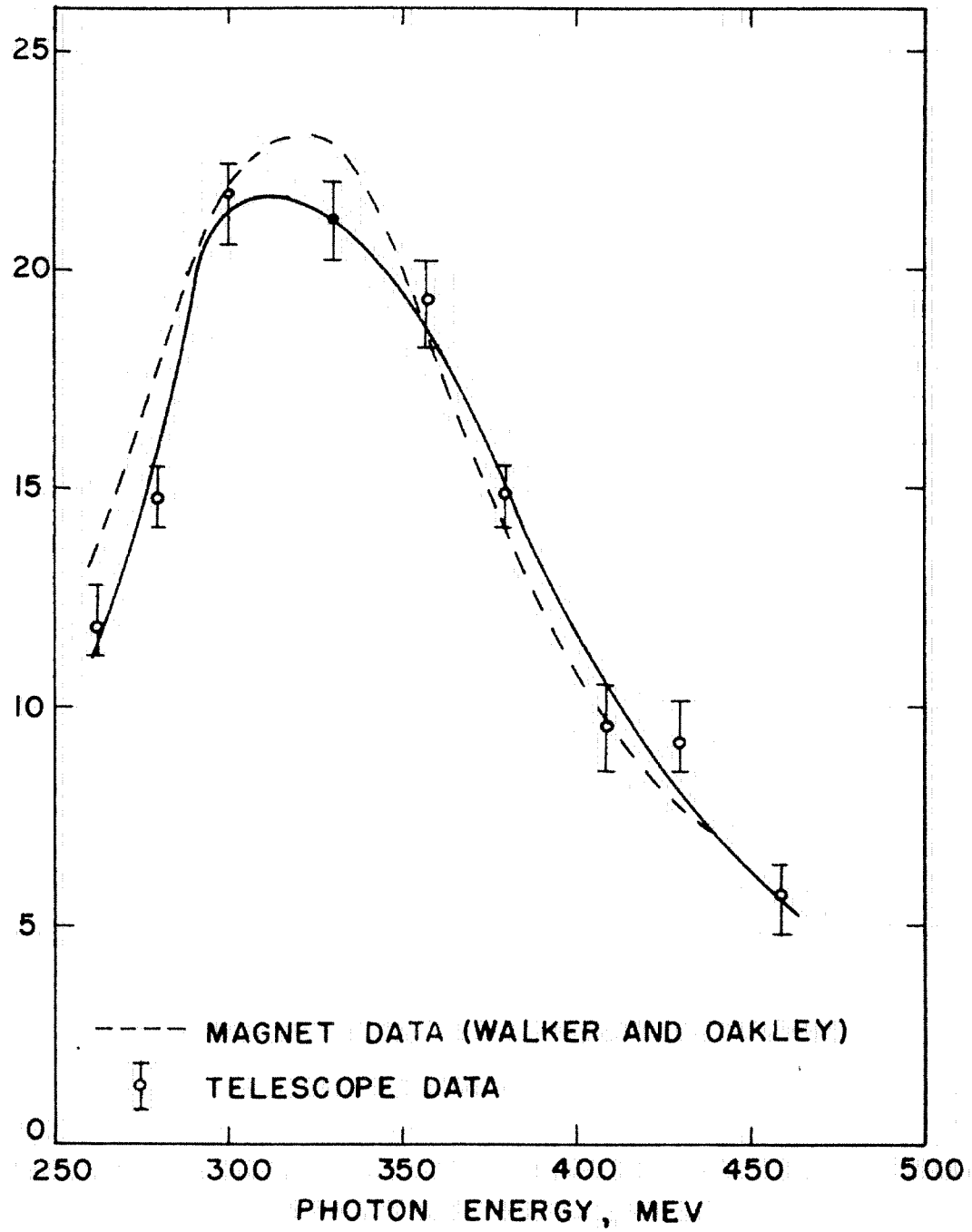

DIFFERENTIAL CROSS SECTION FOR THE REACTION $\gamma + P \rightarrow P + \pi^{\circ}$ AT A PROTON ANGLE OF 29.7° MAGNET DATA IS SHOWN FOR COMPARISON UNITS ARE MICROBARNS / STERADIAN.

Figure 9

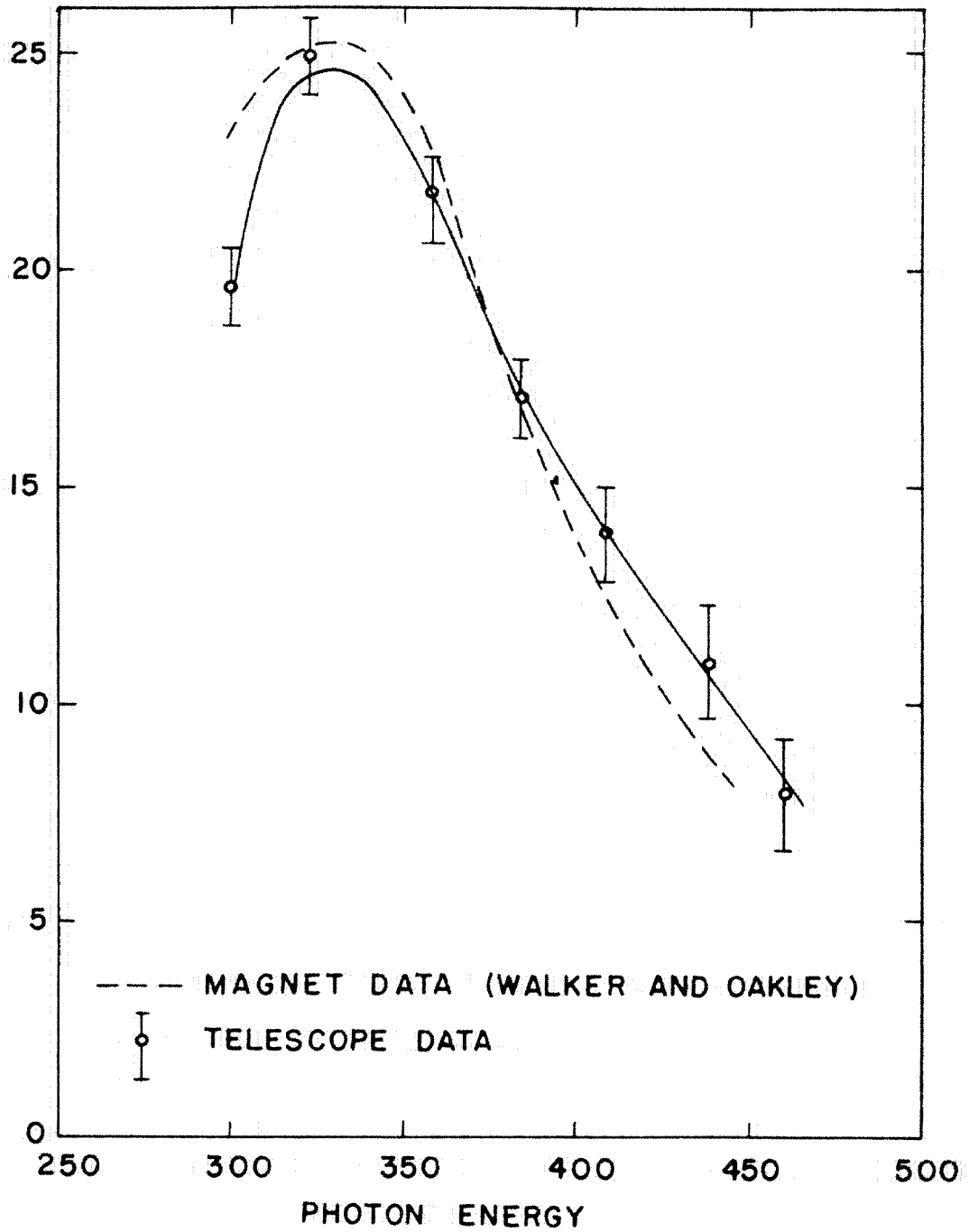

DIFFERENTIAL CROSS SECTION FOR THE REACTION $\gamma + P \rightarrow P + \pi^{\circ}$ AT A PROTON ANGLE OF 41.2°
MAGNET DATA IS SHOWN FOR COMPARISON
UNITS ARE MICROBARNS/STERADIAN.

Figure 10

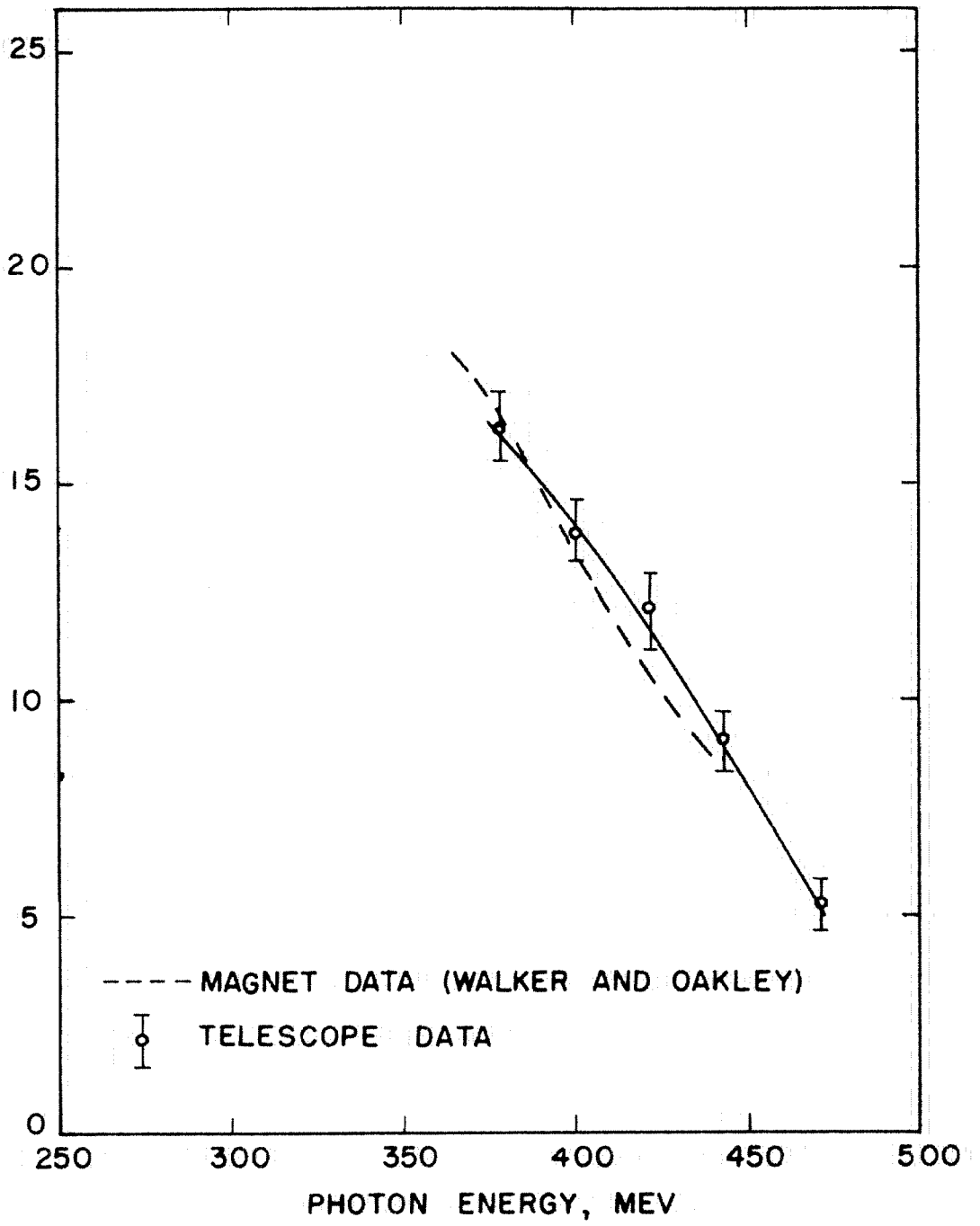

DIFFERENTIAL CROSS SECTION FOR THE REACTION $\gamma + P \rightarrow P + \pi^{\circ}$ AT A PROTON ANGLE OF 51.8° MAGNET DATA IS SHOWN FOR COMPARISON UNITS ARE MICROBARNS/STERADIAN.

Figure 11

through copper. A more complete discussion of the counting rate formula is given in the section describing the deuterium calculation. With the above formula the π^o meson production cross section from hydrogen can be calculated. The corrections discussed in the preceding section were applied to the data to obtain N/bip. The average and maximum values of the corrections are shown in the following table.

Correction	Maximum value	Average value
Background	- 33 °/o	- 17 °/o
Absorption	+ 16 °/o	+ 6.5 °/o
Accidentals	- 8 °/o	- 2 °/o
Deadtime	+ 5.8 °/o	+ 2 °/o
Slit edge	- 5.2 °/o	- 2 °/o

The cross section for π^o production from hydrogen is shown in figures 9, 10 and 11. The dashed curves were drawn by Oakley and Walker through their data at proton angles of 29^o, 40.5^o, and 50.3^o. It is seen that there is good agreement between the two experiments. The sources of error common to both experiments are: the beam monitoring equipment, the measurement of the synchrotron energy, and the hydrogen density measuring equipment.

Absolute errors which apply to all points, and which are not shown on the cross section points are: beam calibration 7 °/o , telescope geometry 5 °/o, hydrogen density 3 °/o, synchrotron energy 0.4 °/o. These combine to give a 9 °/o probable error in absolute cross section, but these errors do not apply to the

photoproton ratios. The sources which contribute to the errors shown on the individual points are: hydrogen and background counting statistics, uncertainty in proton peak limits, absorption correction ($\pm$ 5%o of the correction), telescope angle (+ 0.3°), ΔR (2%o, 3%o, or 5%o depending on A_3), range energy relations (1%o + .01 cm of copper).

The angular distribution coefficients obtained from this experiment are given in the table below. In parenthesis are the coefficients given by Corson, Peterson, and McDonald (8), obtained by combining their photographic plate data with the data of Oakley and Walker. Units are microbarns per steradian.

	Photon Energy		
Coefficient	380 mev	420 mev	460 mev
A	17.8 ± 0.9 (18.0 ∓ 0.7)	12.6 ± 1.2 (11.7 ∓ 0.6)	8.35 ± 1.3 (7.3 ± 0.6)
B	1.7 ± 2.0 (2.6 ∓ 0.9)	2.7 ± 2.4 (2.7 ∓ 0.7)	0.9 ± 2.6 (2.7 ∓ 0.7)
C	-14.0 ± 4.8 (-10.9 ∓ 1.2)	-11.2 ± 5.9 (-7.3 ∓ 1.1)	-13.2 ± 6.3 (-4.2 ∓ 1.0)

The statistical errors overlap the Oakley-Walker coefficients, except for the C coefficient at 460 mev. Our C coefficient is more negative than theirs, but the statistical errors on C are large because our data is all obtained within 26° of 90° in the center of mass system. Since we have data at only three angles

the angular distribution coefficients are not overdetermined, and a least squares fit was not possible.

VII. RESULTS OF THE DEUTERIUM PHOTOPROTON MEASUREMENT

The photoproton counting rate was adjusted by subtracting the photodisintegration contribution which has been discussed, to obtain the photoproton counting rate from meson producing reactions. This deuterium counting rate was divided by the hydrogen counting rate and multiplied by twice the hydrogen to deuterium density ratio, to obtain the photoproton ratio per nucleus. This ratio is plotted in figures 12, 13 and 14. Also shown (dashed curve) is the deuterium to hydrogen photoproton ratio as calculated from the π^- and π^o cross sections of a free proton and neutron at rest. This effort to correlate the present experiment with previous experiments was not completely successful, as can be seen by the dashed curves. It was then decided to calculate the effect that the motion of the neutron and proton in the deuterium nucleus would have on the photoproton ratio predicted by the free nucleon cross sections. This calculation has been described in part V and the results are shown in figures 12, 13 and 14 (solid curve). The agreement between the predicted and measured deuterium to hydrogen photoproton ratio has been improved, especially in regard to the energy dependence of the ratio. However there is still an amplitude discrepancy of about 15%. This discrepancy is discussed further in part X, where a possible cause is also discussed.

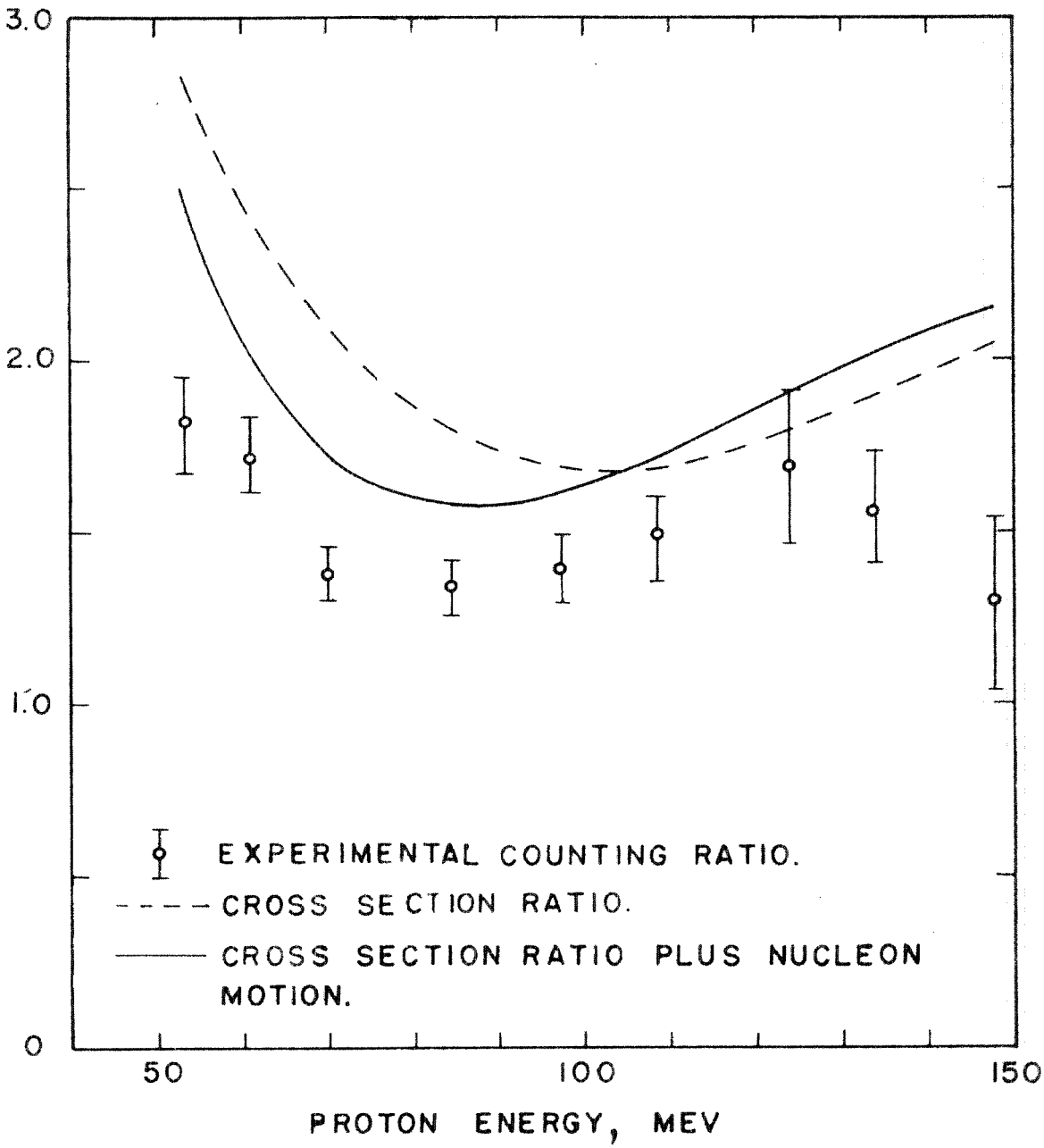

PRODUCTION OF PHOTOPROTONS FROM DEUTERIUM RELATIVE TO HYDROGEN. PHOTO-DISINTEGRATION PROTONS ARE EXCLUDED. $\theta_p = 29.7°$

Figure 12

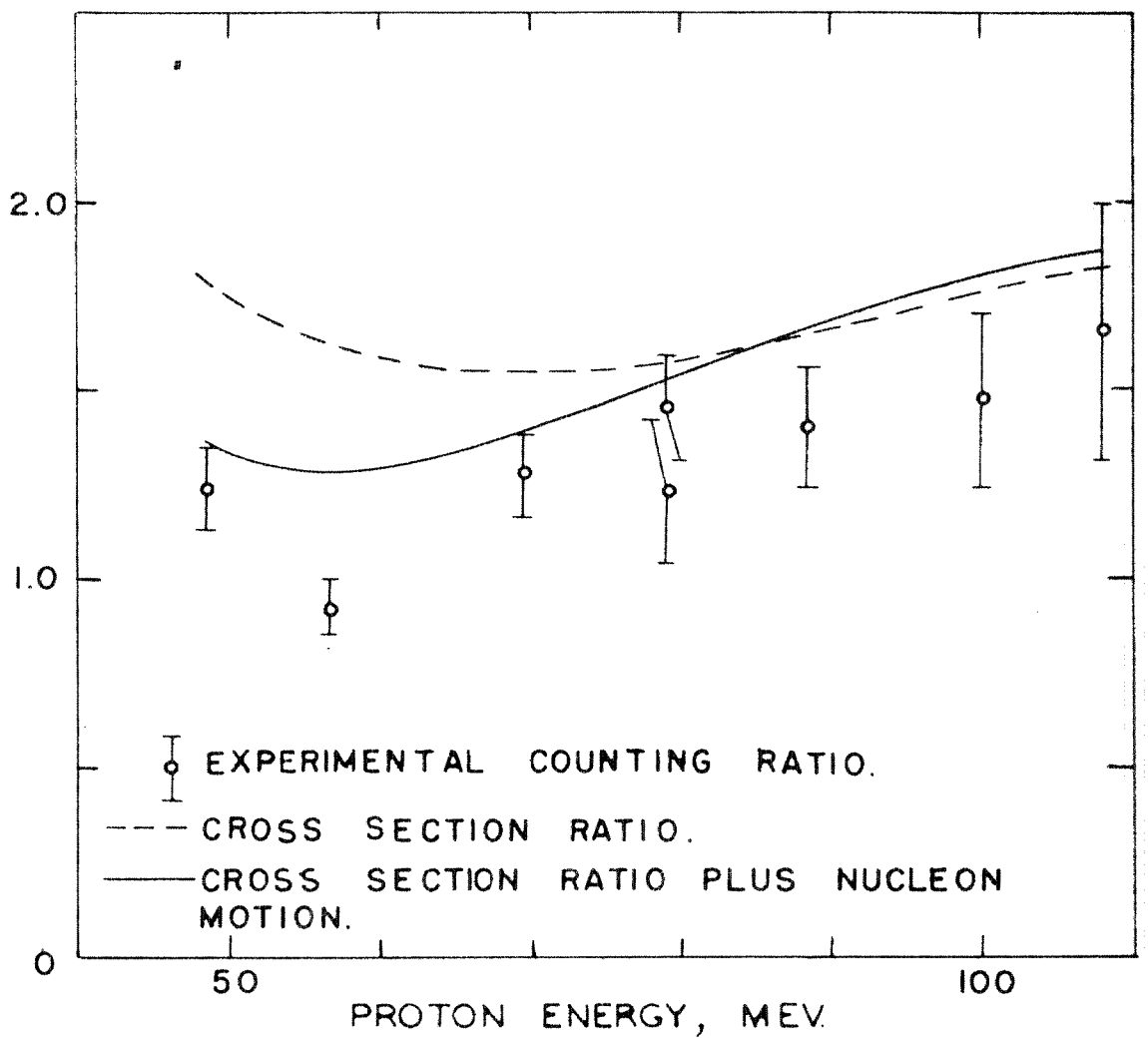

PRODUCTION OF PHOTOPROTONS FROM DEUTERIUM RELATIVE TO HYDROGEN. PHOTO-DISINTEGRATION PROTONS ARE EXCLUDED. $\theta_p = 41.2°$

Figure 13

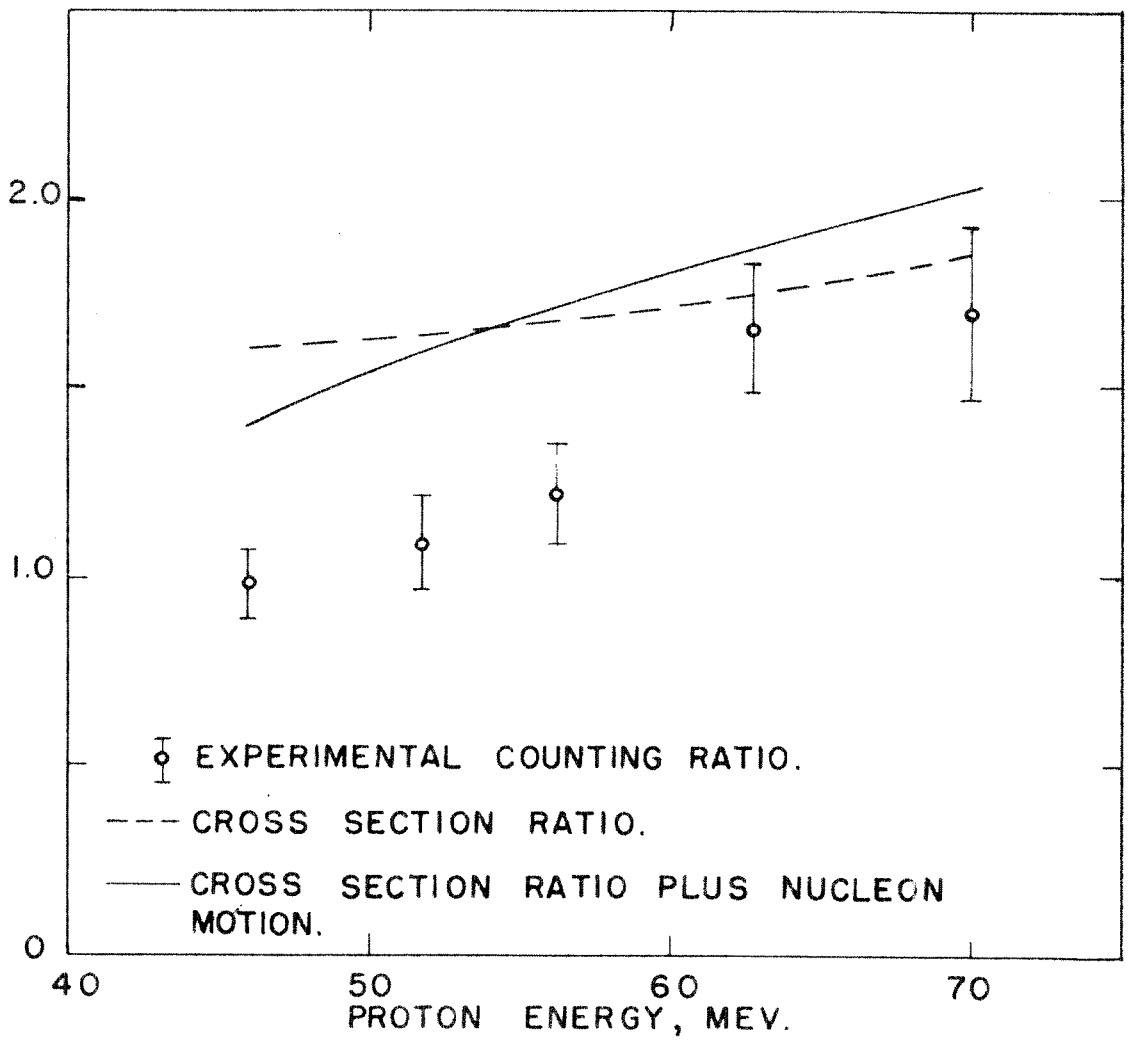

PRODUCTION OF PHOTOPROTONS FROM DEUTERIUM RELATIVE TO HYDROGEN. PHOTO DISINTEGRATION PROTONS ARE EXCLUDED. $\theta_p = 51.8°$

Figure 14

VIII. APPLICATION OF THE DEUTERON CALCULATION TO THE KECK-LITTAUER EXPERIMENT

An interesting experiment involving the deuteron has been performed by James Keck and Raphael Littauer. The interest lies mainly in the unexplained discrepancy between the theoretical and experimental values of the recoil proton energy from π-meson production. In the experiment deuterium was bombarded by 310 mev bremsstrahlung and 56 mev mesons were detected at 90° to the photon beam, in coincidence with the recoil proton. The energy spectrum and the angular distribution of the recoil protons was measured. The angular distribution was found to be as expected from the spectator theory with smearing due to nuclear motions included, however the energy spectrum had very definitely a higher energy peak than was expected from this theory.

It was felt that it might be of interest to apply the Datatron program, previously discussed, to this problem. The program was set up with the condition that a 56 mev meson was observed at 90° to the photon beam. The Datatron then computed, for each of the two hundred possible motions of the target neutron, the energy and direction of the proton recoil. As the weighting function only varied $\pm$ 8% for the two hundred events, it was assumed that the events had equal weight. From the telescope and target geometry (15) the angular resolution function in the azimuthal direction was calculated. This together with the angular resolution curve for the θ (polar angle) direction provided a basis for discarding events in which the proton could not have entered the

counter. It was required that the recoil proton satisfy these two conditions: $|\phi| \leq 23^{o}$, $20^{o} \leq \theta \leq 40^{o}$. One hundred and twelve of the two hundred events satisfied this condition. Their energy distribution is shown in figure 15. The average energy of these protons is 44 mev and the median energy is 43 mev. Four of the successful protons had an energy of over 80 mev and are not shown on the histogram. It seems accidental that there are no events with an energy of 40 mev. It is interesting to note that if the target neutron was at rest the recoil proton would be at 30^{o} with an energy of 40 mev. The theoretical and experimental proton spectra from Keck and Littauer are also presented in figure 15. From the histogram it is found that the peak is the order of 5 mev higher than the theoretical peak of Keck and Littauer, but it is about 6 mev lower than the experimental peak. This difference is still three times the telescope energy calibration uncertainty ($\pm$ 5%), so although the discrepancy has been reduced it has not been eliminated.

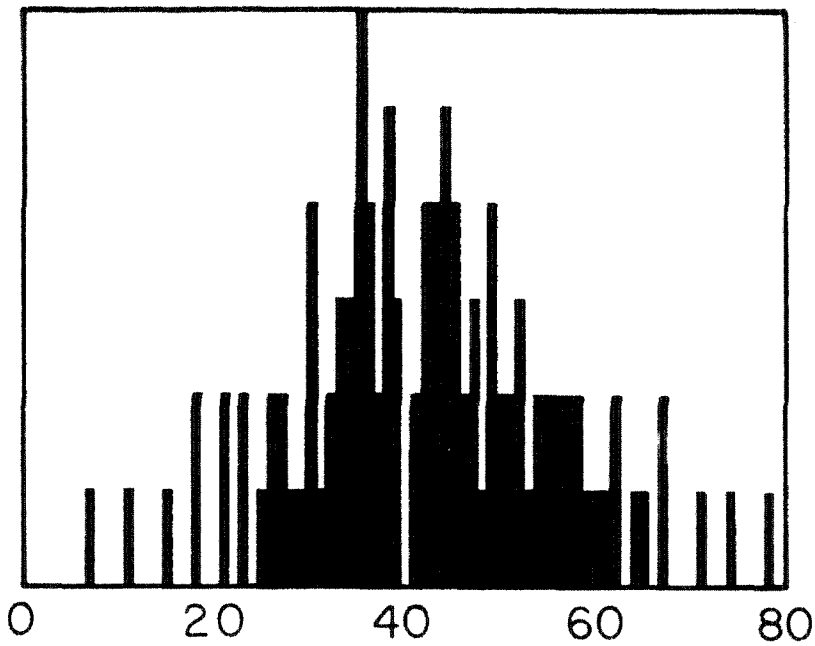

ENERGY DISTRIBUTION OF THE SUCCESSFUL EVENTS OF THE DATATRON CALCULATION. AVERAGING OVER 8 MEV INTERVALS PRODUCES THE HISTOGRAM BELOW

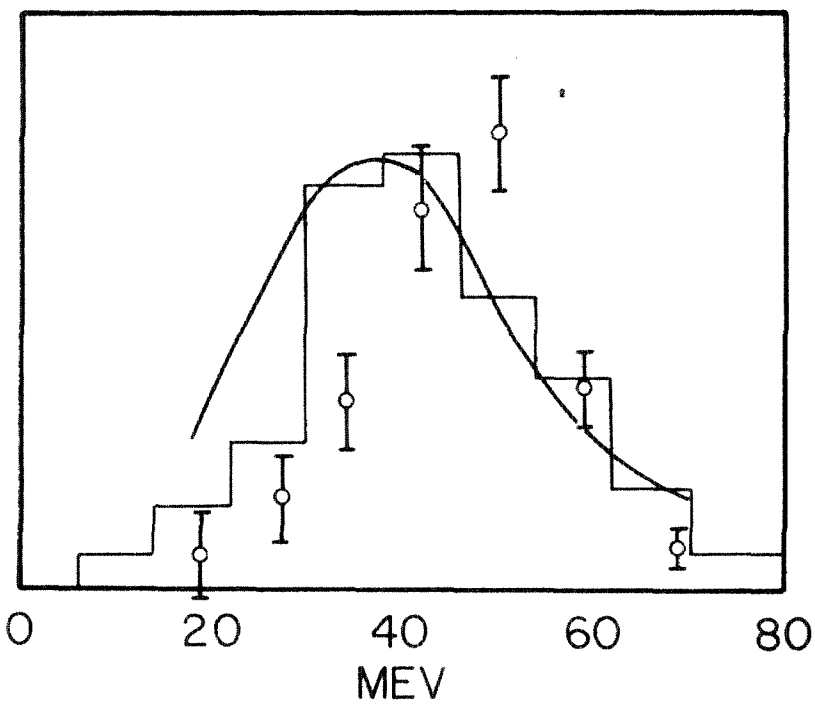

THEORETICAL AND EXPERIMENTAL PROTON ENERGY DISTRIBUTION FROM KECK AND LITTAUER

Figure 15

IX. APPLICATION OF THE DEUTERON CALCULATION TO MESON RATIO EXPERIMENTS

Sands et al. (12) have measured the ratio of positive meson production from deuterium and hydrogen. This experiment should be a good subject for the deuteron dynamics calculation, in the range where the recoil neutron has high momentum (>300 mev/c) so that the exclusion principle and the density of final states do not restrict positive meson production from deuterium. This calculation has the advantage that only one, well known, cross section enters; where in the photoproton case there were two cross sections involved and one (the negative pi) was not as thoroughly known as is the positive pi cross section. Sands, Teasdale and Walker (6) have measured the negative to positive pion ratio from deuterium at the same energies and angles as the positive pion ratio. It required only a little more computer time to calculate the effect of the neutron motion in the deuteron on negative pion production. This can be combined with the positive pion ratio to obtain the effect of nucleon motion on the negative to positive ratio. The positive meson ratio is shown in figures 16, 17 and 18 with the experimental points of Sands et al. The calculation and the experiment agree although it would be a better test of the calculation if the experimental statistics were better.

The ratio of negative pion production from a neutron in deuterium and a neutron at rest (figure 19) is of interest because it justifies the original assumption that we could take the measured negative pion cross section from deuterium as equal to the

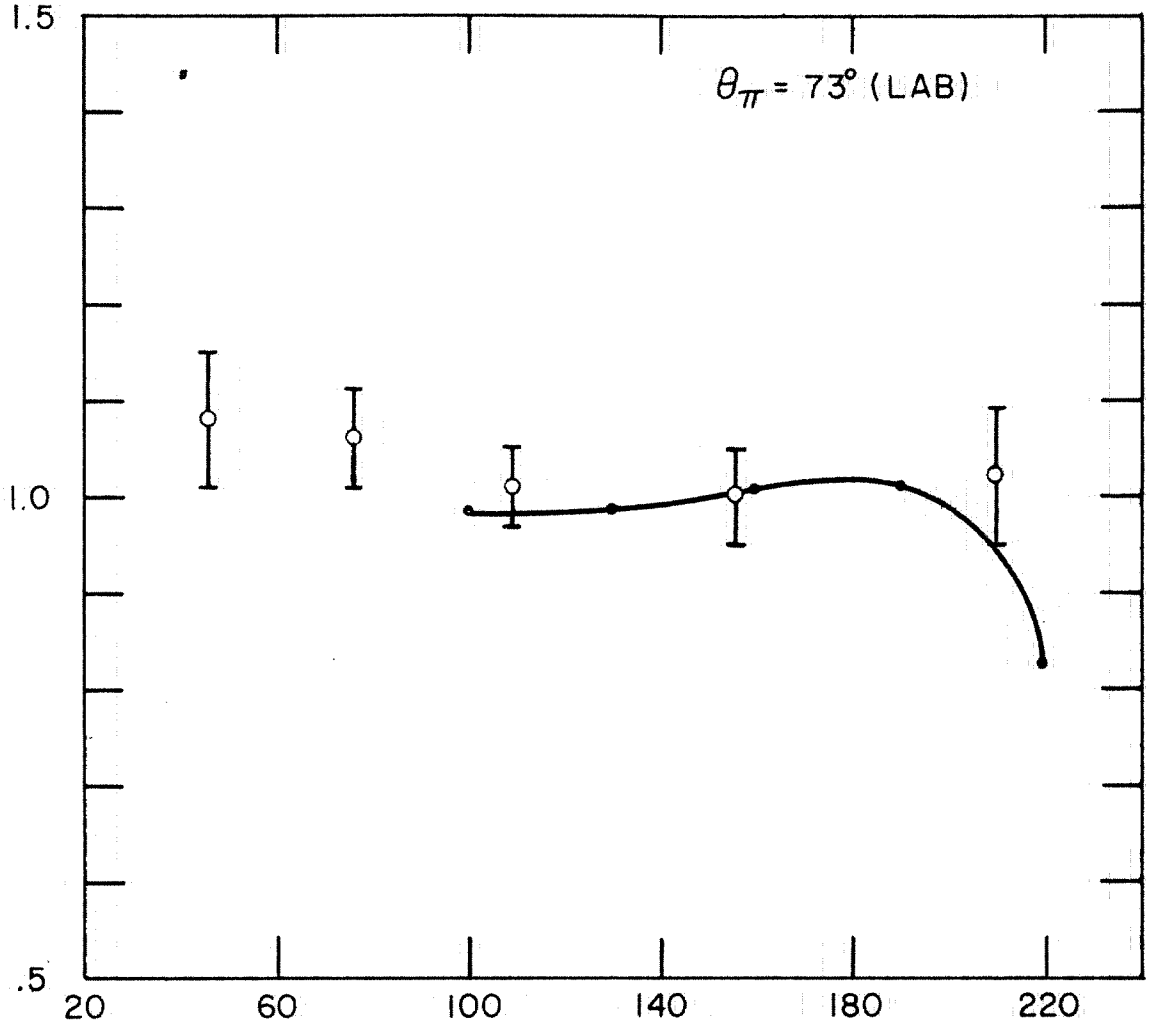

POSITIVE MESON PRODUCTION FROM DEUTERIUM RELATIVE TO HYDROGEN. THE EXPERIMENTAL POINTS ARE THOSE OF SANDS ET AL.

Figure 16

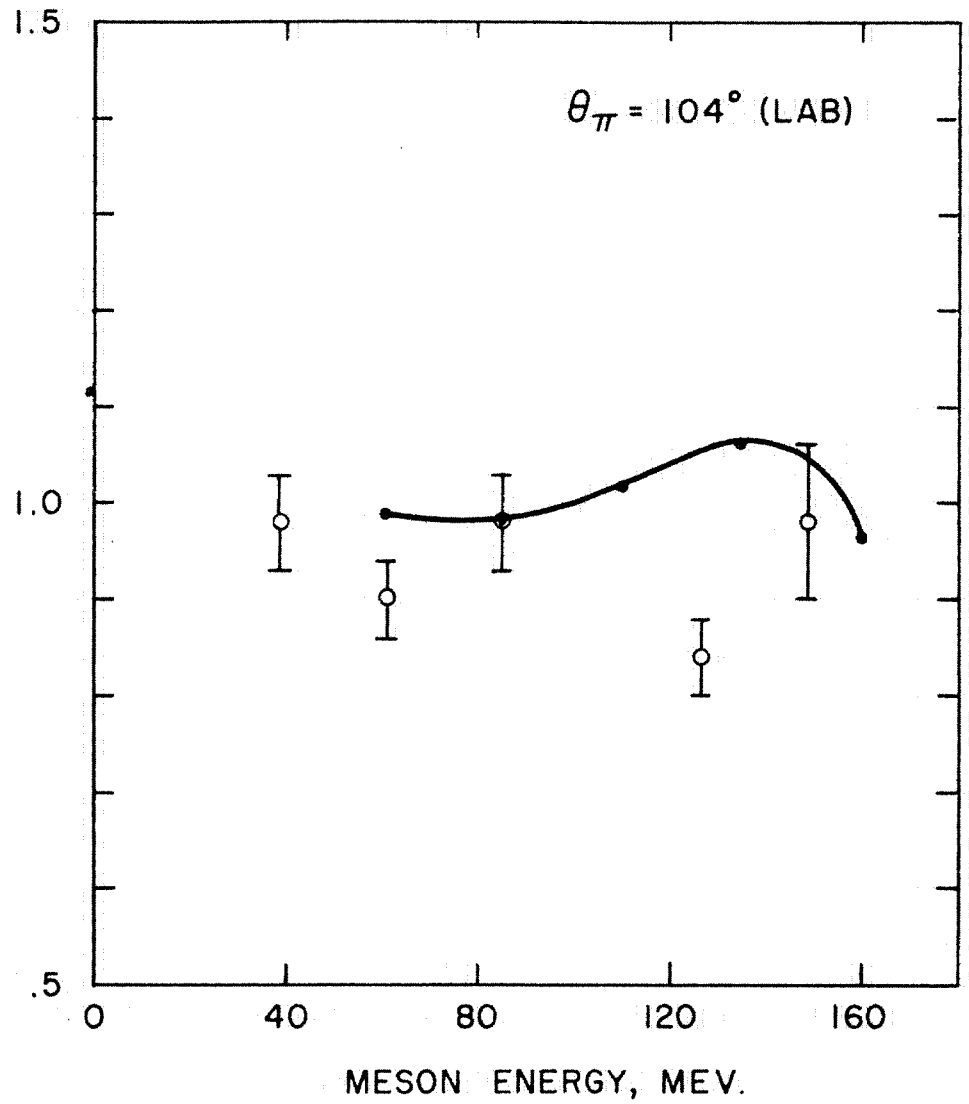

POSITIVE MESON PRODUCTION FROM DEUTERIUM RELATIVE TO HYDROGEN. THE EXPERIMENTAL POINTS ARE THOSE OF SANDS ET AL.

Figure 17

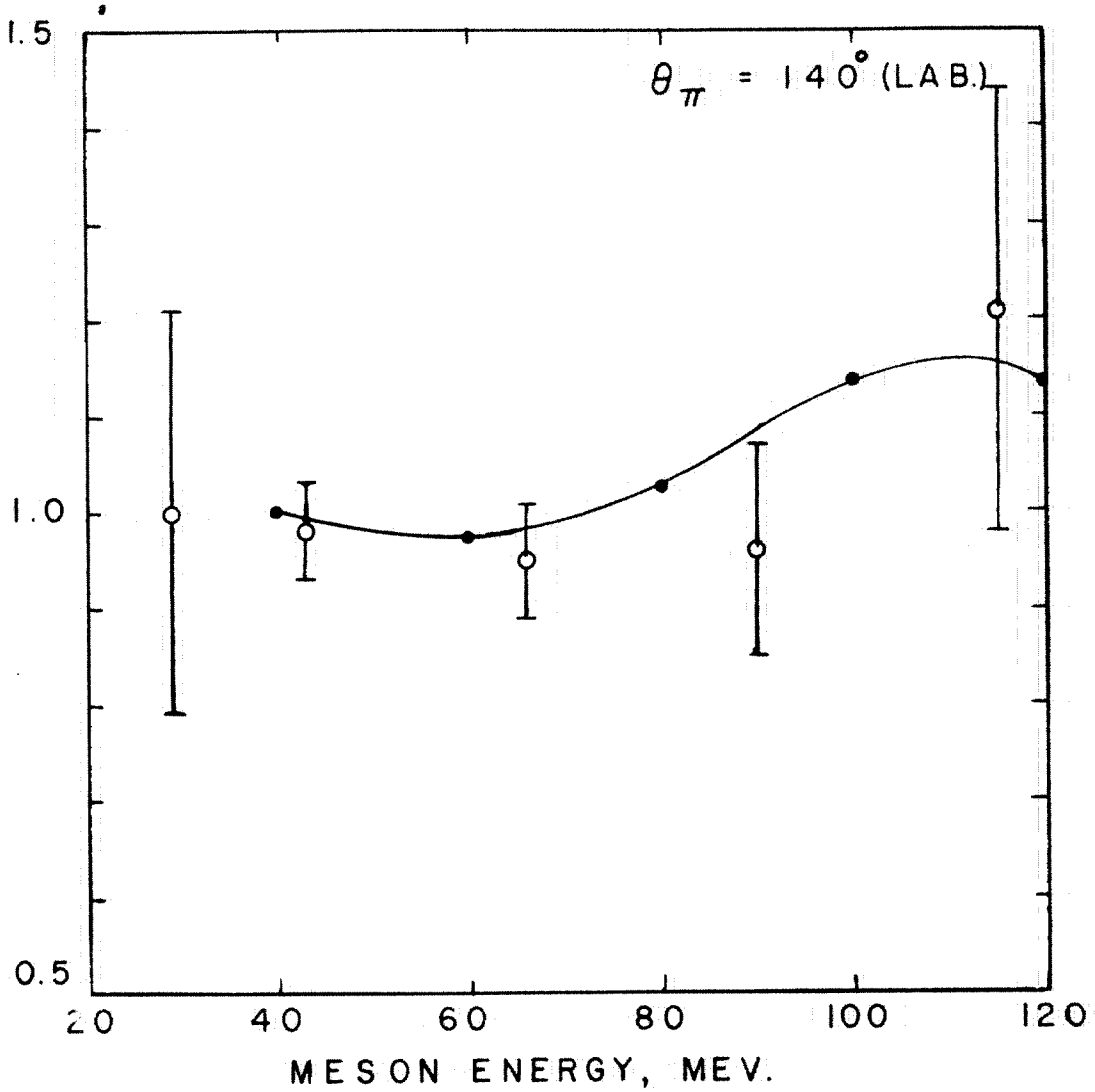

POSITIVE MESON PRODUCTION FROM DEUTERIUM RELATIVE TO HYDROGEN. THE EXPERIMENTAL POINTS ARE THOSE OF SANDS ET AL.

Figure 18

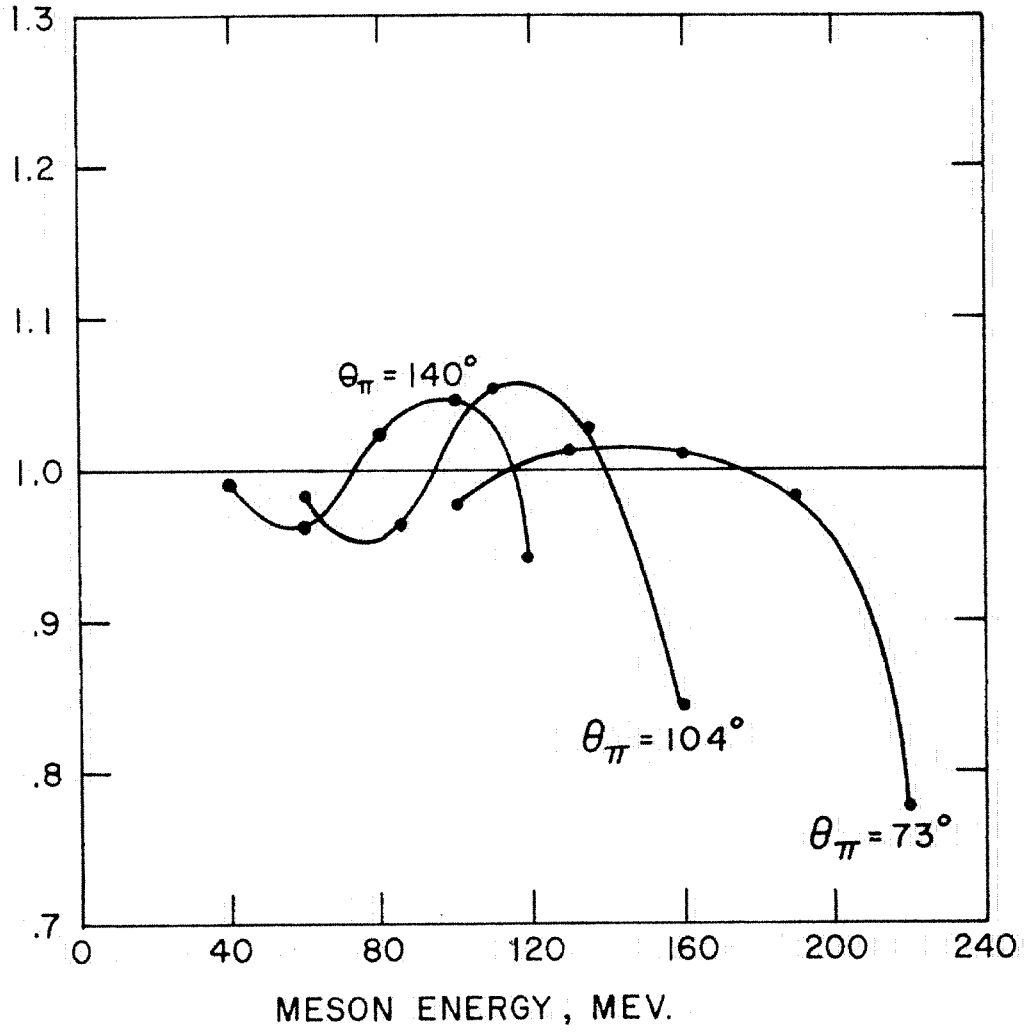

NEGATIVE MESON PRODUCTION FROM DEUTERIUM RELATIVE TO PRODUCTION FROM NEUTRONS AT REST.

Figure 19

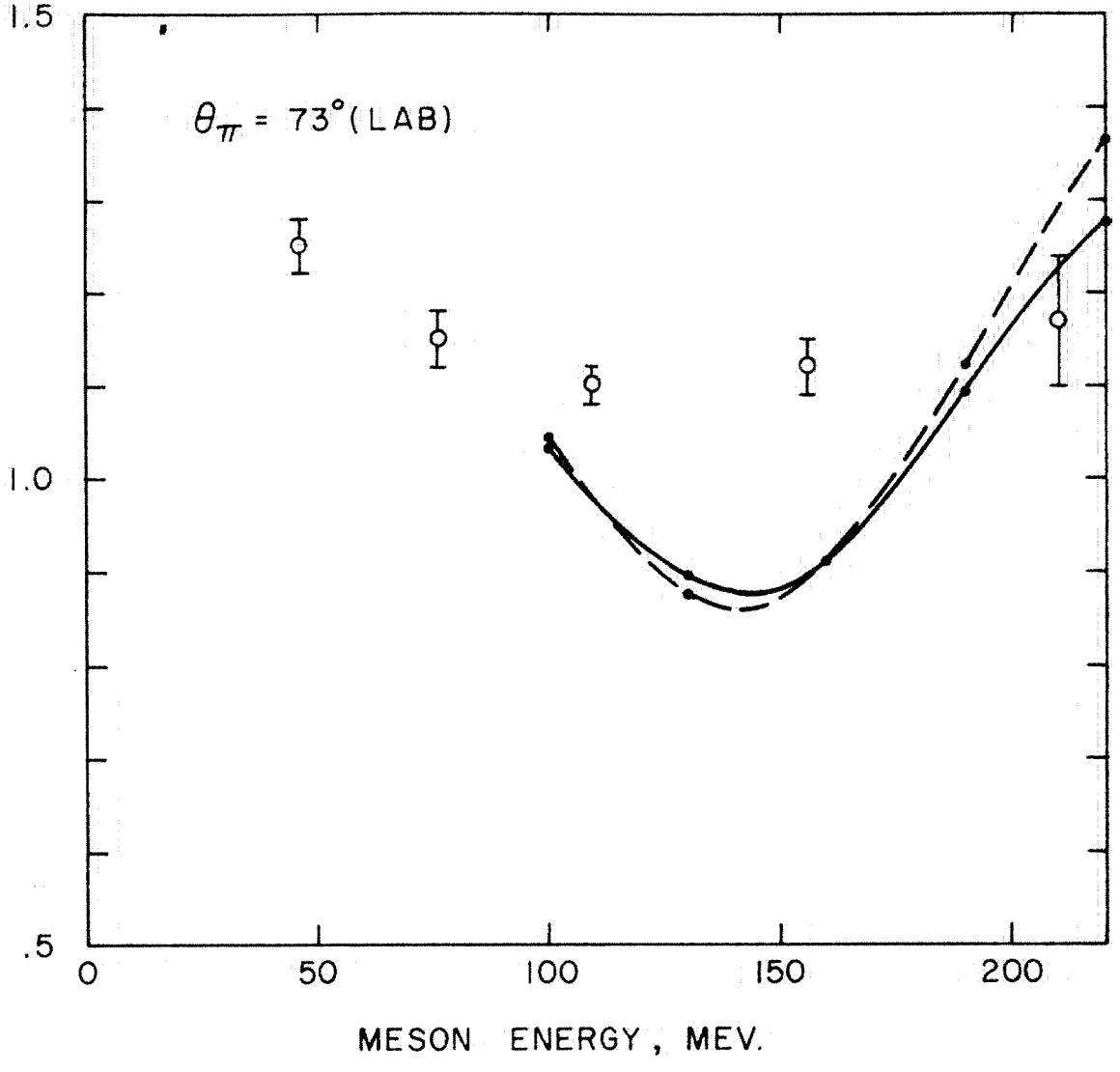

NEGATIVE TO POSITIVE RATIO OF PHOTOMESONS FROM DEUTERIUM. EXPERIMENTAL POINTS ARE FROM SANDS, TEASDALE, AND WALKER. DASHED CURVE IS CROSS-SECTION RATIO (SEE TEXT). SOLID CURVE SHOWS SMEARING EFFECT DEUTERIUM NUCLEON MOTION.

Figure 20

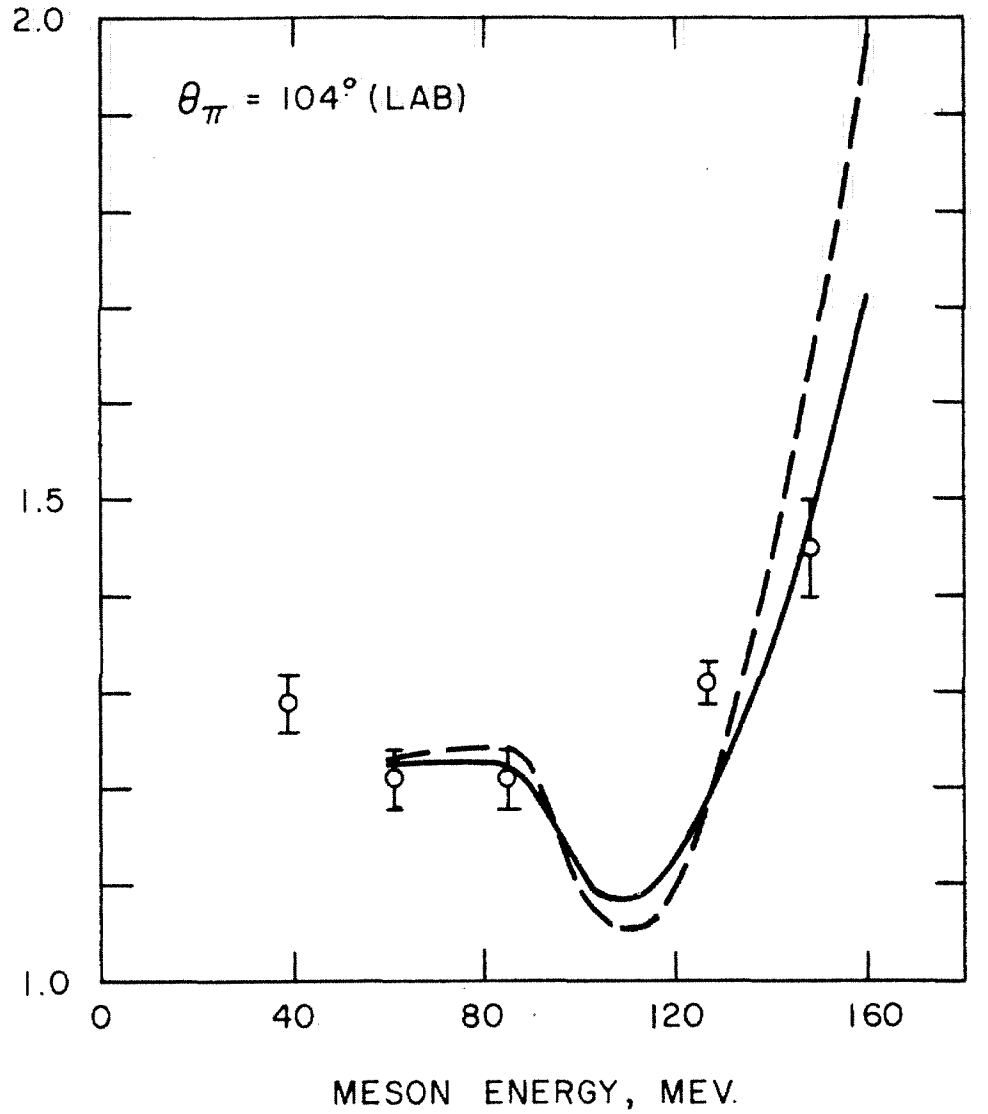

NEGATIVE TO POSITIVE RATIO OF PHOTOMESONS FROM DEUTERIUM. EXPERIMENTAL POINTS ARE FROM SANDS, TEASDALE, AND WALKER. DASHED CURVE IS CROSS SECTION RATIO (SEE TEXT). SOLID CURVE SHOWS SMEARING EFFECT DEUTERIUM NUCLEON MOTION.

Figure 21

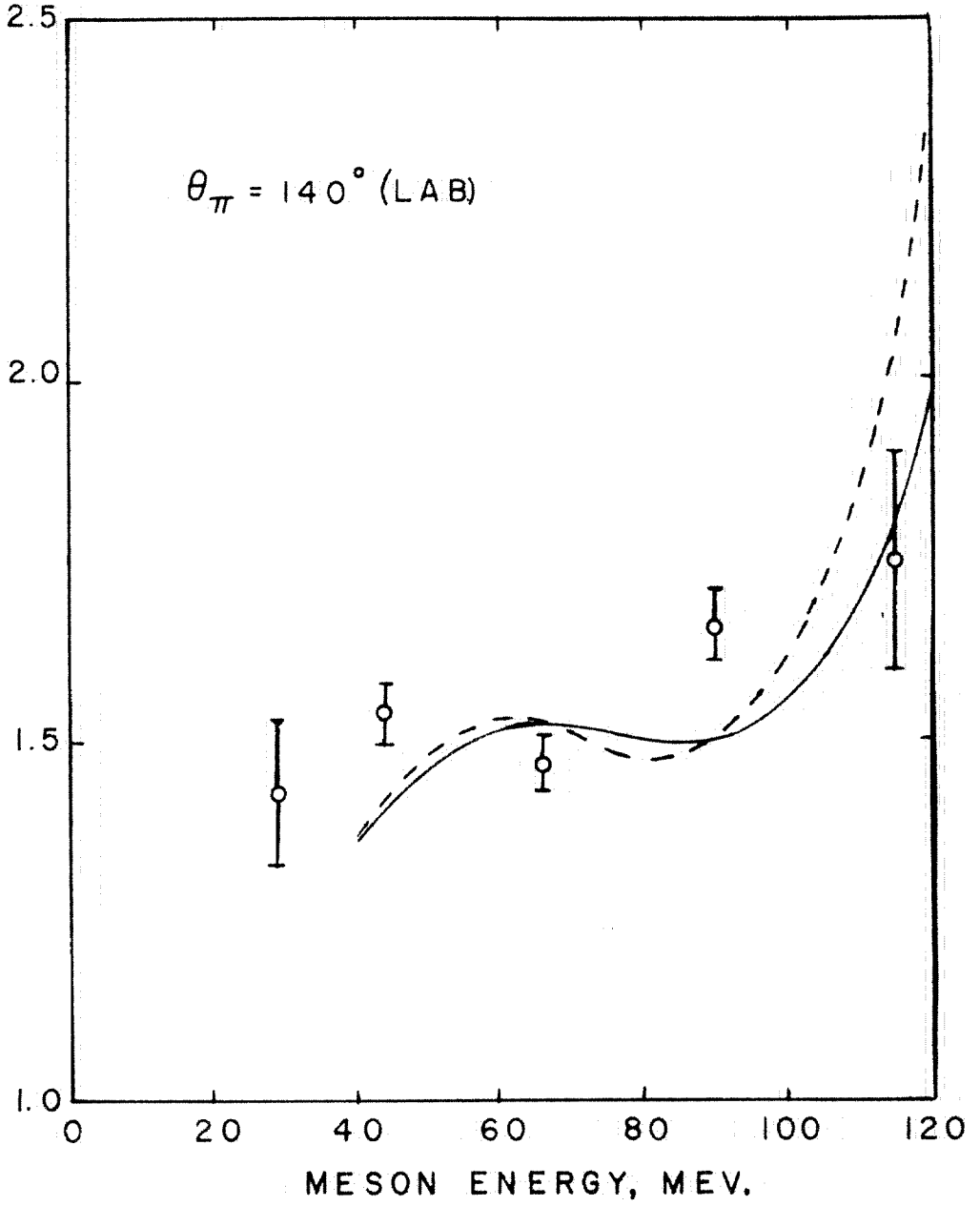

NEGATIVE TO POSITIVE RATIO OF PHOTO-MESONS FROM DEUTERIUM. EXPERIMENTAL POINTS ARE FROM SANDS, TEASDALE AND WALKER. DASHED CURVE IS CROSS SECTION RATIO (SEE TEXT). SOLID CURVE SHOWS SMEARING EFFECT DEUTERIUM NUCLEON MOTION.

Figure 22

negative pion cross section of neutrons at rest. The calculation showed that the ratio was within 6% of unity in the regions where the negative pion cross section was measured. At the upper end of the bremsstrahlung spectrum this ratio decreases and then abruptly becomes infinite at the meson energy corresponding to a 500 mev photon. Figures 20, 21 and 22 show the negative to positive ratio from deuterium. The difference between the ratio for nucleons at rest (dashed curve) and the ratio for nucleons in deuterium (solid curve) is the smearing effect of nuclear motion. The agreement of the curves with the experimental points is not significant, as the experimental points were used to obtain the cross section coefficients used in the calculation*. Unfortunately the smearing is not sufficient to account for the discrepancy between theory and experiment at a meson angle (lab) of 140° encountered by Watson, et al. (18). This ratio was calculated from the two preceding ratios using the identity:

$$\left(\frac{\sigma_D^-}{\sigma_D^+}\right) = \frac{\left(\frac{\sigma_D^-}{\sigma_N^-}\right)}{\left(\frac{\sigma_D^+}{\sigma_H^+}\right)} \left(\frac{\sigma_N^-}{\sigma_H^+}\right),$$

where σ is the cross section for photoproduction of the pion whose charge is given by the superscript, from a deuteron, proton or neutron as indicated by the subscript. The ratios $\left(\frac{\sigma_D^-}{\sigma_N^-}\right)$ and $\left(\frac{\sigma_D^+}{\sigma_H^+}\right)$ tend to behave similarly, and would be equal if σ_N^- was proportional to σ_H^+ at all energies and angles.

*The poor fit of the cross section ratio to the experimental points results from forcing a fit of the form $A+B\cos\theta'+C\cos^2\theta'$ to the π^- cross section.

X. DISCUSSION OF RESULTS

The results of the neutral pion cross section measurement (figures 8, 9 and 10) are not as extensive as those of Oakley and Walker, but the agreement provides a useful consistency check, since the two methods employed different means of detecting the recoil protons.

The application of the deuteron program to the Keck-Littauer experiment has resulted in improved agreement with experiment; however, it is difficult to say whether the remaining disagreement is significant.

The calculated deuterium photoproton ratios agree with experiment as far as shape is concerned (figures 12, 13 and 14), with the exception of the high energy points at 29.7°, but the calculated ratios are too large by about $15^{\circ}/o$. Two possible causes of this discrepancy will be discussed. The first is the negative pion cross section. If the value of this cross section used in the calculation was too large it would make the calculated photoproton ratio too large also. This cross section was obtained by taking the product of the negative to positive pion ratio from deuterium, the positive pion ratio from deuterium to hydrogen, and the positive pion cross section from hydrogen. The possibility of cumulative errors make this method uncertain, and a probable error of $\pm$ $15^{\circ}/o$ was estimated for the negative pion cross section used in the calculation. About $45^{\circ}/o$ of the photoprotons are due to negative meson production.

The second cause for the discrepancy between theory and experiment is that a meson produced on one nucleon may be

absorbed by the other nucleon, leading to photodisintegration. In a very recent paper Wilson (24) quotes a probability of 0.11 for this process, and calculates the photodisintegration cross section of deuterium, which agrees exceedingly well with experiment. An effort was made to confirm this absorption coefficient by examining the various deuterium to hydrogen ratio experiments.

The π^+ deuterium to hydrogen ratio has been measured at Cornell (25, 26), M.I.T. (27), Stanford (28), and at the University of California at Berkeley (29), with bremsstrahlung in the vicinity of 300 mev. The expected value of the deuterium to hydrogen π^+ ratio (see for example (29)) produced by 300 mev bremsstrahlung differs from unity for two reasons in addition to the reabsorption probability. In the lower energy region where the recoil neutron has low momentum there is a reduction of the available phase space due to the exclusion principle, unless the spin of the proton is flipped in the interaction so that the two neutrons are in different spin states. At higher energies where this effect becomes unimportant there is the effect of the proximity of the bremsstrahlung upper limit. A particular energy of meson can be produced by a variety of photon energies because of the momentum distribution of the nucleons in deuterium. As the meson energy at which the ratio is observed is increased, the deuterium to hydrogen ratio decreases because some of the required photon energies are above the bremsstrahlung upper limit. The ratio would be expected to decrease to

about one half and then to increase rapidly to infinity as the photon energy required to produce mesons from hydrogen reaches the breamsstrahlung upper limit.

The experimental values of the π^+ deuterium to hydrogen ratio from the 300 mev machines are inconclusive as regards evidence for or against the 11% reabsorption figure. This is due to poor statistics and disagreement between different experiments. The π^+ deuterium to hydrogen ratio from 500 mev bremsstrahlung has been measured at Cal Tech (12) and is shown in figures 16, 17 and 18. The theoretical curves include the effect of the bremsstrahlung spectrum shape, and the recoil momentum is large enough so that the spin states do not matter. It is seen that if the curves were decreased by 11% the agreement with experiment would be improved at 104° and 140° but would be worsened at 73°. The net agreement would remain about the same.

The deuterium to hydrogen π° ratio would also be affected by the reabsorption of mesons in deuterium. It is extremely difficult to do an experiment where a π° of a particular energy and angle is observed, so one must be content with the ratio of decay gamma rays from the π° mesons from deuterium and hydrogen. An experiment of this kind done by the photon difference method (the subtraction of two runs of different machine energy) is not directly comparable to the π^+ ratios previously discussed, as it gives the ratio for monoenergetic photons and all energies of the meson, while the π^+ ratio was for a specific meson energy

produced by a bremsstrahlung spectrum. Since π^o mesons can be produced from neutrons as well as from protons there is the possibility of interference effects, which might alter the angular distribution.

This experiment has been performed by Cocconi and Silverman (30) at Cornell with 310 mev bremsstrahlung and by Keck, Tollestrup and Bingham (31) at Cal Tech with 500 mev bremsstrahlung using the photon difference method. Averaging the 310 mev data from Cornell over meson energies and angles we find that the π^o production per nucleon in deuterium is 10% less than from hydrogen, with statistical errors of about 5%. The Cal Tech data is consistent with this 10% reduction at 73^o and 140^o but the ratio is larger at 30^o, which Keck et al. suggest may be an interference effect. Typical errors are 5%.

From these π^+ and π^o deuterium to hydrogen ratios it can be said that they are consistent with the 11% reabsorption probability, but that they do not provide strong evidence for it. The best evidence comes not from the meson ratio experiments where one must look for an 11% difference between measured quantities, but from the photodisintegration of the deuteron at the higher energies, which is almost entirely caused by this effect.

If we accept 11% as the probability for the reabsorption of a meson produced in deuterium, then the π^o cross section used to calculate the photoproton ratio must be reduced by this amount. The π^- cross section which was used depended on the deuterium to

hydrogen π^+ ratio, and if this is smaller than the measured values which were used, then this cross section should be slightly reduced also. Taking into account the uncertainty of the π^- cross section we can say that the various meson ratio and photoproton ratio experiments are consistent with the known meson cross sections and the spectator model of the deuteron, if we assume an 11% probability of meson reabsorption leading to photodisintegration of the deuteron.

APPENDIX I

DETAILS OF THE DEUTERIUM CALCULATION

Two hundred momenta were selected to represent the spherically symmetric motions of the target nucleons. The perpendiculars to the faces of a regular icosahedron form a set of twenty symmetric directions. These directions are given in the following table, where the polar coordinate system has been chosen with its axis parallel to the incident photons. The orientation of the icosahedron with respect to the $\phi = 0$ plane, which contains the recoil proton, is selected to avoid degeneracy. Degeneracy is possible because the dynamics are symmetric about the $\phi = 0$ plane, hence a nucleon with momentum direction (ϕ, θ) will give the same result as one with the direction $(-\phi, \theta)$. Because of this symmetry the icosahedron is oriented so that when the hemisphere below the $\phi = 0$ plane is reflected into the upper hemisphere, the twenty directions will not be degenerate, but will be equally spaced azimuthally. Because of this symmetry both ϕ and θ are between 0 and π. For each of the four values of θ_n there are five values of ϕ_n.

θ_n	ϕ_n
37.39°	18°
79.19	54
100.81	90
142.61	126
	162

Ten equally probable momenta for each of these twenty directions

are calculated from the deuteron wave function. We will need the momentum transformation equation:

$$\Phi(P,\theta,\phi) = \frac{1}{(\sqrt{2\pi}\hbar)^3}\int_0^{\pi}\int_0^{2\pi}\int_0^{\infty} \Psi(r,\theta,\phi)\, e^{-\frac{i}{\hbar}\mathbf{P}\cdot\mathbf{r}}\, r\,\sin\theta\, d\theta\, r\, d\phi\, dr,$$

where: $\Psi(r,\theta,\phi) = \sum_{\ell} U_{\ell}(r) \sum_{m=-\ell}^{\ell} \alpha_{\ell m}\, Y_{\ell m}(\theta,\phi)$ = the deuteron spatial wave function with the property that:

$$\sum \alpha_{\ell m}^2 = 1.$$

$Y_{\ell m}(\theta,\phi)$ = normalized spherical harmonic,

and: $\Phi(P,\theta,\phi)$ = the deuteron momentum wave function,

$\mathbf{P}\cdot\mathbf{r}$ = Pr cosβ where β is the angle between $\mathbf{P}$ and $\mathbf{r}$.

An identity which we will need is:

$$e^{-i\frac{Pr}{\hbar}\cos\beta} = \sum_{N=0}^{\infty} (-i)^N (2N+1)\, j_N\left(\frac{Pr}{\hbar}\right) P_N(\cos\beta),$$

where $P_N(\cos\beta)$ is the Legendre polynomial of order N and j_N is the spherical Bessel function defined in terms of half integral Bessel functions as follows:

$$j_N\left(\frac{Pr}{\hbar}\right) = \sqrt{\frac{\pi\hbar}{Pr}}\; J_{N+\frac{1}{2}}\left(\frac{Pr}{\hbar}\right).$$

Another identity which we will use is:

$$P_N(\cos\beta) = \frac{4\pi}{2N+1} \sum_{M=-N}^{N} Y_{NM}^{*}(\theta,\phi)\, Y_{NM}(\theta_P,\phi_P),$$

where β is the angle between the r vector (θ ,φ) and the P vector (θ_p, ϕ_p). Substituting in the expression for Φ we obtain:

$$\Phi = \sum_{\ell} \frac{1}{(\sqrt{2\pi}\hbar)^3} \int_0^{\pi}\int_0^{2\pi}\int_0^{\infty} U_\ell(r)\, r^2 dr \sum_{m=-\ell}^{\ell} \alpha_{\ell m} Y_{\ell m}(\theta,\phi) \sum_{N=0}^{\infty} (-i)^N (2N+1)\, j_N\left(\frac{pr}{\hbar}\right)$$

$$\frac{4\pi}{2N+1} \sum_{M=-N}^{N} Y^*_{N,M}(\theta,\phi)\, Y_{NM}(\theta_p,\phi_p)\, \sin\theta\, d\theta\, d\phi.$$

The integral over θ and ϕ give zero except when $N = \ell$ and $M = m$ so the only terms left are:

$$\Phi(P) = \sum_{\ell} \sum_{m=-\ell}^{\ell} \frac{4\pi}{(\sqrt{2\pi}\hbar)^3} Y_{\ell m}(\theta_p,\phi_p)\, \alpha_{\ell m} (-i)^\ell \int_0^{\infty} U_\ell(r)\, j_\ell\left(\frac{pr}{\hbar}\right) r^2 dr.$$

The probability density function $\rho(p)$ is obtained by averaging $\Phi^* \Phi$ over all angles since there is no special orientation of the target deuterons:

$$\rho(P) = \int_0^{2\pi}\int_0^{\pi} \Phi^*(P,\theta_p,\phi_p)\, \Phi(P,\theta_p,\phi_p)\, P \sin\theta_p\, d\phi_p\, P\, d\theta_p,$$

$$\rho(P) = \frac{2}{\pi\hbar} \sum_{\ell} \left[\frac{p}{\hbar} \int_0^{\infty} U_\ell(r)\, j_\ell\left(\frac{pr}{\hbar}\right) r^2 dr\right]^2.$$

Since we are concerned only with S and D states where $\ell = 0$ or 2 we use:

$$j_0\left(\frac{pr}{\hbar}\right) = \frac{\hbar}{pr} \sin\frac{pr}{\hbar},$$

$$j_2\left(\frac{pr}{\hbar}\right) = \frac{\hbar}{pr}\left\{\left[3\left(\frac{\hbar}{pr}\right)^2 - 1\right] \sin\frac{pr}{\hbar} - 3\frac{\hbar}{pr}\cos\frac{pr}{\hbar}\right\}.$$

We are interested in two wave functions.

The Hulthén wave function:

$$U_o = \frac{A}{r}\left(e^{-\alpha r} - e^{-\beta r}\right),$$

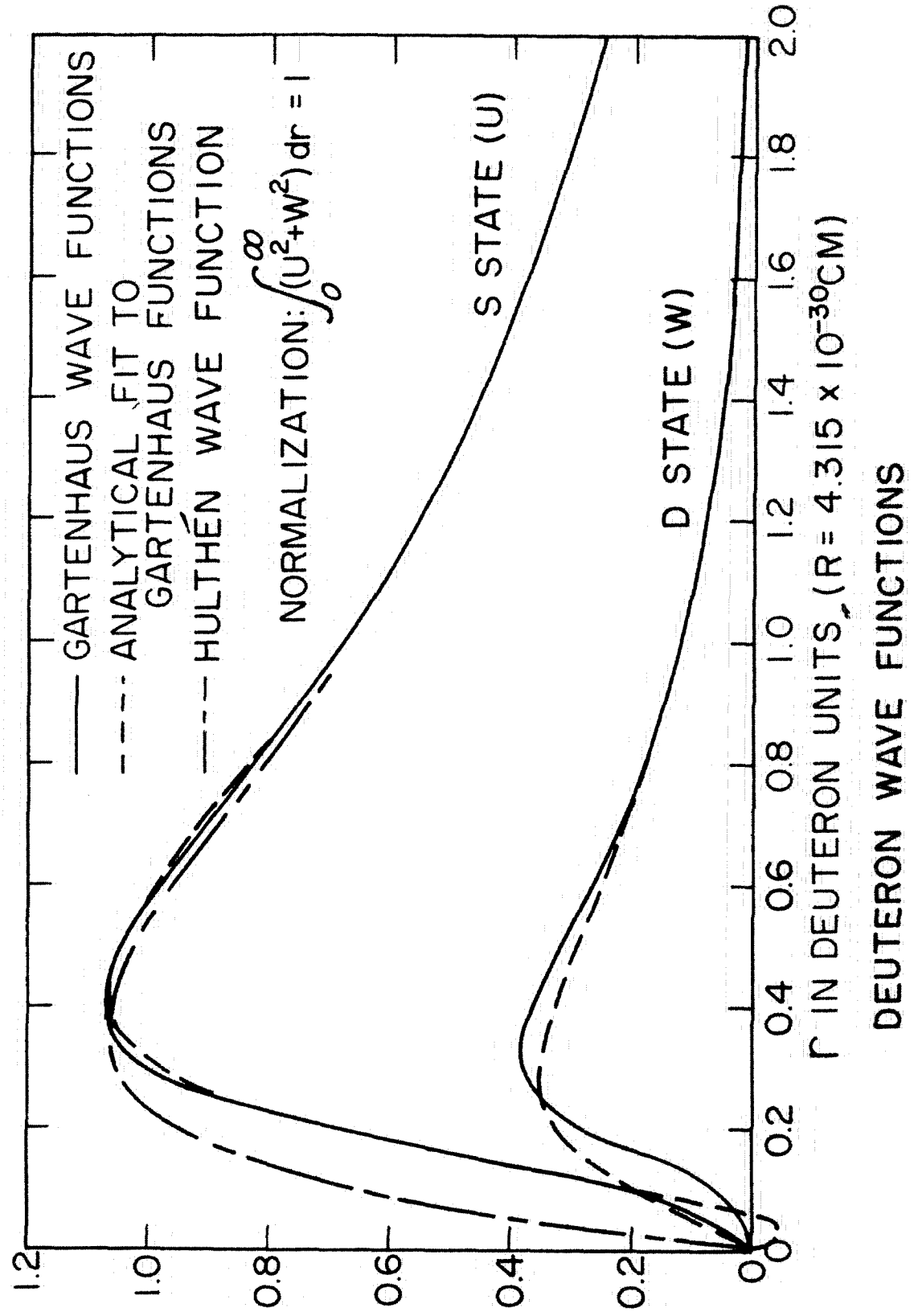

Figure 23

Figure 23

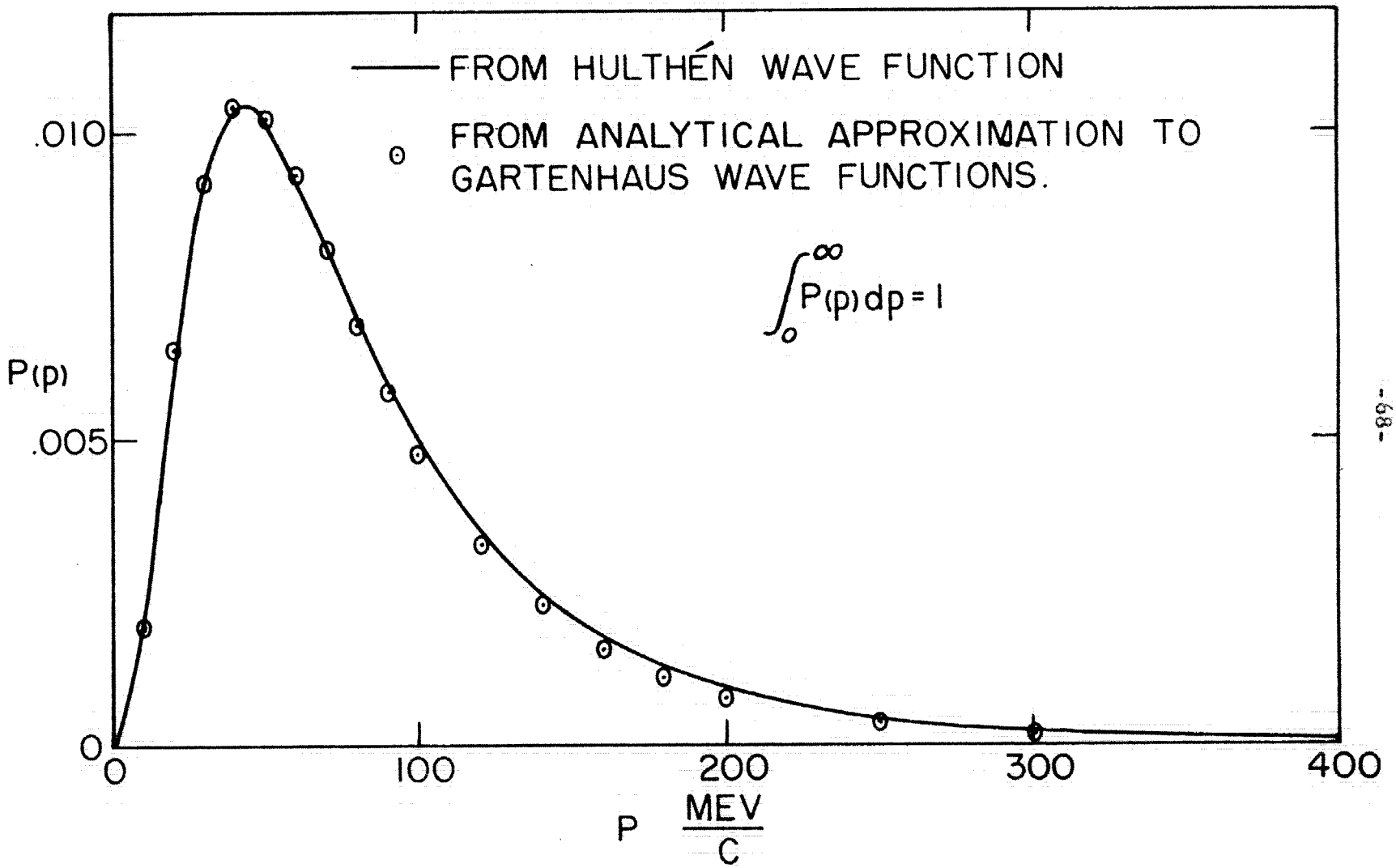

NUCLEON MOMENTUM DISTRIBUTION IN THE DEUTERON

Figure 24

$$\int_o^\infty U_o^2 r^2 \, dr = 1, \quad \alpha = .231 \times 10^{13} \text{ cm}^{-1}, \quad \beta = 1.41 \times 10^{13} \text{ cm}^{-1}.$$

The Gartenhaus (7) wave function:

$$U_o = \frac{U}{r}, \qquad U_2 = \frac{W}{r}, \qquad \int_o^\infty (U^2 + W^2) dr = 1.$$

The Gartenhaus wave functions together with the following approximate analytical fits are shown in figure 23:

$$U = 1.85 \left[e^{-r} - 13.4 e^{-10r} + 12.4 e^{-11r} \right], \text{(r in deuteron units)}$$

$$W = .89 \left[e^{-2r} - e^{-6.3r} \right].$$

The poor fit to the D state wave function was tolerated because the total D state contribution is only 7 °/o, Both the Gartenhaus and the Hulthen wave functions were transformed to obtain the probability density function. The results are shown in figure 24. The ten momenta were chosen so that 5 °/o of the area under the momentum distribution curve was to the left of the first value, 15 °/o of the area for the second value and 95 °/o for the tenth value. The momenta obtained are:

20.0 mev/c	73.0 mev/c
32.5	87.0
42.2	106
51.5	133
61.5	185

Derivation of K, $\left.\frac{dK}{dT}\right|_{\cos\theta_2}$ for the case in which the target

nucleon is not at rest. Both a spherical and a rectangular coordinate system are used, oriented as follows:

X axis: $\theta_x = 0$,

Y axis: $\theta_y = \frac{\pi}{2}$, $\phi_y = 0$,

Z axis: $\theta_z = \frac{\pi}{2}$, $\phi_z = \frac{\pi}{2}$.

Units will be used such that the velocity of light is unity. The following quantities will be needed:

$\underline{K}$ is the photon momentum ($K = K_x$ defines the X axis.);

$\underline{P}_n$ is the target nucleon momentum ($\phi_n = 0$ defines the XY plane.);

P_1, θ_1, ϕ_1, P_2, θ_2, ϕ_2 are the momentum and direction of the products;

M_1, E_1, M_2, E_2, M_n, E_n are the masses and total energies of the particles.

A useful identity is: $E = \sqrt{P^2 + M^2} = T + M$.

Writing the equations for the conservation of energy and momentum, we obtain:

$$K + E_n = E_1 + E_2 = \sqrt{M_1^2 + P_1^2} + E_2,$$

X direction: $K + P_n\cos\theta_n = P_1\cos\theta_1 + P_2\cos\theta_2$,

Y direction: $P_n\sin\theta_n = P_1\sin\theta_1\cos\phi_1 + P_2\sin\theta_2\cos\phi_2$,

Z direction: $0 = P_1\sin\theta_1\sin\phi_1 + P_2\sin\theta_2\sin\phi_2$.

We wish to eliminate P_1, θ_1, ϕ_1 from these equations. If we

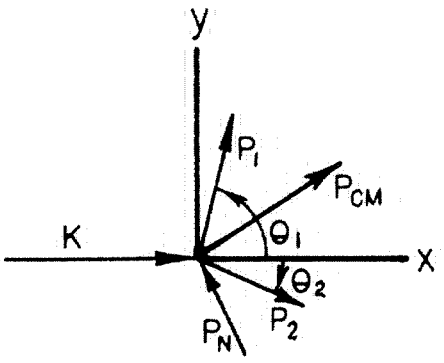

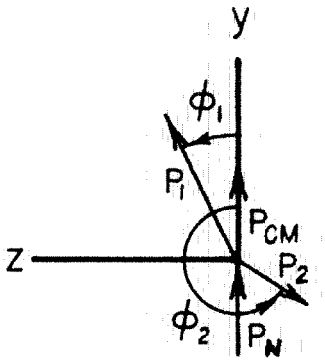

COORDINATE SYSTEM FOR DERIVATION OF K

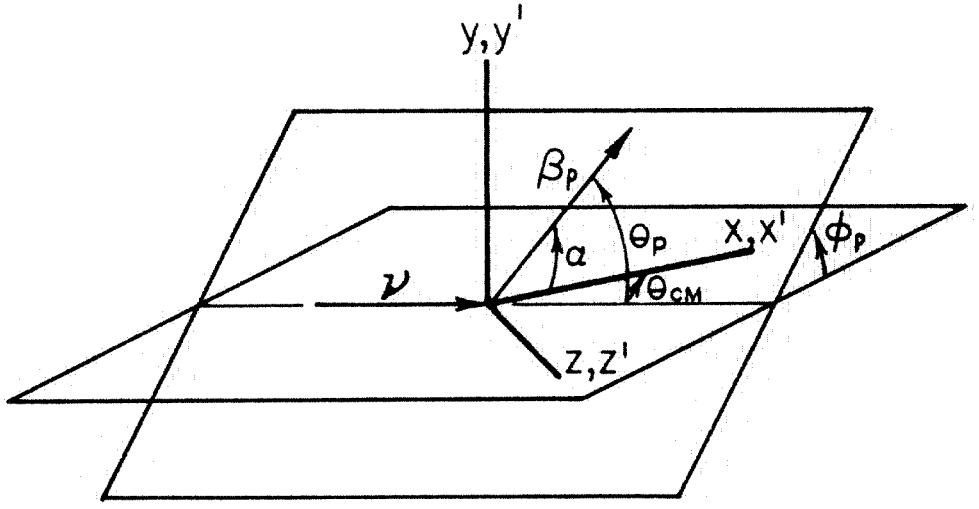

COORDINATE SYSTEM FOR DERIVING Cos δ & Cos α

Figure 25

transpose to the left side all but terms in P_1 in the momentum equations then we may square and add the three momentum equations giving us an expression for P_1^2 which we may substitute into the energy equation, thus eliminating the undesired variables and giving an equation which may be solved for K:

$$K = \frac{(E_n-E_2)^2-M_1^2-P_2^2-P_n^2+2P_2P_n(\cos\theta_2\cos\theta_n+\sin\theta_n\sin\theta_2\cos\phi_2)}{2(E_2-E_n+P_n\cos\theta_n-P_2\cos\theta_2)}.$$

Considering K as a function of T_2 and $\cos\theta_2$ we wish to find $\frac{\partial K}{\partial T_2}$ with $\cos\theta_2$ held constant where T_2 is the kinetic energy of M_2. The variables depending on T_2 are: $E_2 = T_2 + M_2$ and $P_2 = \sqrt{T_2^2 + 2M_2T_2}$. If the differentiation is carried out we obtain:

$$\frac{\partial K}{\partial T_2} = \frac{P_2(E_n-E_2)+K(P_2-E_2\cos\theta_2)+E_2P_2-P_n(\cos\theta_n\cos\theta_2+\sin\theta_n\sin\theta_2\cos\phi_2)}{P_2(E_n-P_n\cos\theta_n-E_2+P_2\cos\theta_2}.$$

Calculation of $\left.\frac{\partial\cos\alpha'}{\partial\cos\alpha}\right|_K$.

Choose a laboratory coordinate so that the X axis is parallel to the direction of the center of mass motion, β_{cm}. Pick the Y axis so that the XY plane contains the velocity vector $\underline{\beta}$ of the recoil proton, which makes an angle α with the X axis. Choose a prime coordinate system with axes parallel to the first system, but moving in the positive X direction with a velocity β_{cm} with respect to it. We wish to find $\cos\alpha$ in terms of $\cos\alpha'$, β', and β_{cm}. We now write the velocity transformation equations between the two

systems:

$$\beta_x = \frac{\beta_{cm} + \beta'_x}{1 + \beta'_x\beta_{cm}}, \qquad \beta_y = \frac{\sqrt{1 - \beta_{cm}^2}}{1 + \beta'_x\beta_{cm}}\,\beta'_y,$$

$$\beta'_x = \frac{\beta_x - \beta_{cm}}{1 - \beta_x\beta_{cm}}, \qquad \beta'_y = \frac{\sqrt{1 - \beta_{cm}^2}}{1 - \beta_{cm}\beta_x}\,\beta_y.$$

If we transform $\cos\alpha = \frac{\beta_x}{\beta}$ we obtain:

$$\cos\alpha = \frac{\beta_{cm} + \beta'\cos\alpha'}{\sqrt{\beta_{cm}^2 + \beta'^2 + 2\beta_{cm}\beta'\cos\alpha' - \beta'^2\beta_{cm}^2(1 - \cos^2\alpha')}}.$$

Since β_{cm} and β' depend only on K it is easy to obtain the partial derivative of $\cos\alpha$ with respect to $\cos\alpha'$ with K held constant. We use this result and the transformation equations to obtain the following equation, usually called the solid angle transformation equation:

$$\left.\frac{\partial\cos\alpha'}{\partial\cos\alpha}\right|_K = \frac{\beta^2(1 - \beta_{cm}^2)}{(\beta - \beta_{cm}\cos\alpha)\sqrt{\beta^2 + \beta_{cm}^2 - 2\beta\beta_{cm}\cos\alpha - \beta_{cm}^2\beta^2\sin^2\alpha}}.$$

β is determined by the telescope. β_{cm} and $\cos\alpha$ can be calculated from the center of mass motion.

The center of mass motion. The incident photon is absorbed by the target nucleon to form the center of mass system which moves with a velocity β_{cm} at an angle θ_{cm} to the original photon

direction. Writing the conservation of momentum, we find:

$$K + P_n \cos\theta_n = P_{cm}\cos\theta_{cm}, \qquad P_n \sin\theta_n = P_{cm}\sin\theta_{cm},$$

$$P_{cm} = \sqrt{K^2 + P_n^2 + 2KP_n\cos\theta_n},$$

$$\cos\theta_{cm} = \frac{K + P_n\cos\theta_n}{\sqrt{K^2+P_n^2+2KP_n\cos\theta_n}}, \quad \beta_{cm} = \frac{P_{cm}}{E_{cm}} = \frac{\sqrt{K^2+P_n^2+2KP_n\cos\theta_n}}{K + E_n}.$$

Derivation of $\cos\delta$. Consider a laboratory coordinate system with the X axis in the direction of the center of mass motion, and the XZ plane containing the incident photon direction. Consider the vector ν, whose amplitude is the photon frequency and has the direction of the photon. This vector has the following components:

$$\nu_x = \nu\cos\theta_{cm}, \qquad \nu_z = \nu\sin\theta_{cm}.$$

We can obtain the desired transformation to the center of mass system by considering relativistic contravariant momentum four vector $\nu^\mu = (\nu_x, \nu_y, \nu_z, \nu)$. Upon transforming this four vector we obtain the following equations:

$$\nu_x' = \frac{\nu_x - \beta_{cm}\nu}{1-\beta_{cm}^2} = \frac{\cos\theta_{cm} - \beta_{cm}}{1-\beta_{cm}^2}\nu, \qquad \nu_z' = \nu_z = \nu\sin\theta_{cm},$$

$$\nu' = \nu\frac{1-\beta_{cm}\cos\theta_{cm}}{1-\beta_{cm}^2}.$$

We now wish to find the motion of the recoil proton in the center of mass system. The components of the proton velocity in the laboratory system can be written:

$$\beta_x = \beta_p (\cos\theta_p \cos\theta_{cm} + \sin\theta_p \sin\theta_{cm} \cos\phi_{cm}),$$

$$\beta_y = \beta_p \sin\theta_p \sin\phi_{cm},$$

$$\beta_z = \beta_p (\cos\theta_p \sin\theta_{cm} - \sin\theta_p \cos\phi_{cm} \cos\theta_{cm}).$$

It is now seen that:

$$\cos\alpha = \cos\theta_p \cos\theta_{cm} + \sin\theta_p \cos\phi_{cm} \sin\theta_{cm},$$

where azimuthal angles are measured from the $\phi_p = 0$ plane. Transforming to the center of mass system, we obtain:

$$\beta'_x = \frac{\beta_x - \beta_{cm}}{1 - \beta_x \beta_{cm}}, \qquad \beta'_y = \frac{\beta_y \sqrt{1-\beta_{cm}^2}}{1-\beta_x \beta_{cm}}, \qquad \beta'_z = \frac{\beta_z \sqrt{1-\beta_{cm}^2}}{1-\beta_x \beta_{cm}}.$$

Since δ is the angle between the incident photon and the recoil proton in the center of mass system we may write:

$$\cos\delta = \frac{\gamma' \circ \beta'}{\gamma' \beta'},$$

which gives:

$$\cos\delta = \frac{(\beta_x - \beta_{cm})(\cos\theta_{cm} - \beta_{cm}) + \beta_z \sin\theta_{cm}(1-\beta_{cm}^2)}{(1-\beta_{cm}\cos\theta_{cm}) \sqrt{(\beta_x - \beta_{cm})^2 + (\beta_y^2 + \beta_z^2)(1-\beta_{cm}^2)}}.$$

K_o is the incident photon energy as measured in a coordinate system in which the target nucleon is at rest. The target nucleon is moving with a velocity β_n in a direction θ_n, ϕ_n. We may use the equations previously derived when we transformed the photon to the center of mass system:

$$K_o = K \frac{1 - \beta_n \cos\theta_n}{\sqrt{1 - \beta_n^2}}.$$

The cross section for the production of π^o mesons from free protons has been compiled from three sources. The middle and upper regions are from the data of Oakley and Walker (1) (magnet) and Corson, Peterson, and McDonald (8) (photographic plates), all of this laboratory. This region was also measured in the first part of this experiment, which agreed with the preceding experiments. In the low energy region the data of Mills and Koester (9) of the University of Illinois was used.

The cross section for π^- meson production from neutrons was obtained from the data of Sands et al (6), who counted the π^- mesons produced from deuterium. To justify the use of this data it must be shown that the motion of the neutrons does not significantly influence the measurement of the cross section. The difference in measuring a single nucleon cross section in deuterium by counting the mesons and by counting the recoil protons is shown in figures 6 and 7. Figure 6, as previously explained, shows the smearing effect of the deuterium motions in the case when recoil protons are observed. The Datatron was used to solve the case when this same cross section is measured by counting mesons. The result is figure 6. It is immediately seen that there is much less smearing in the case where the meson is observed. The same Datatron program was used to calculate the ratio of π^- production from neutrons and deuterium. The results are shown in figure 19. These results show that we are justified in using the data of Teasdale et al. to predict the number of recoil protons produced by π^- meson production.

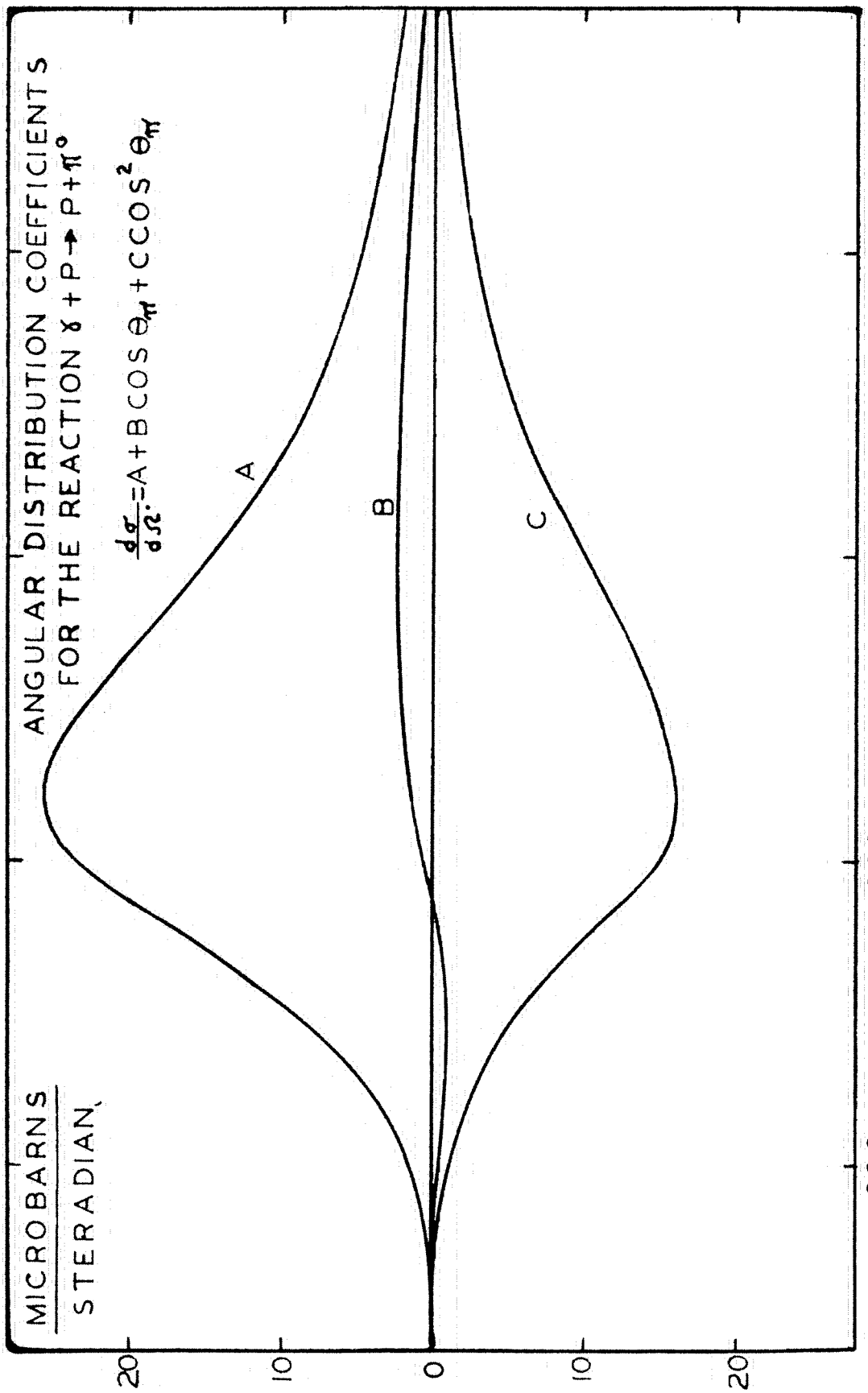
ANGULAR DISTRIBUTION COEFFICIENTS
FOR THE REACTION γ + P → P + π°
dσ/dΩ* = A + B COS θ_π + C COS² θ_π
A
B
C
MICROBARNS / STERADIAN
20
10
0
10
20
200
300
400
500
K MEV

Figure 26

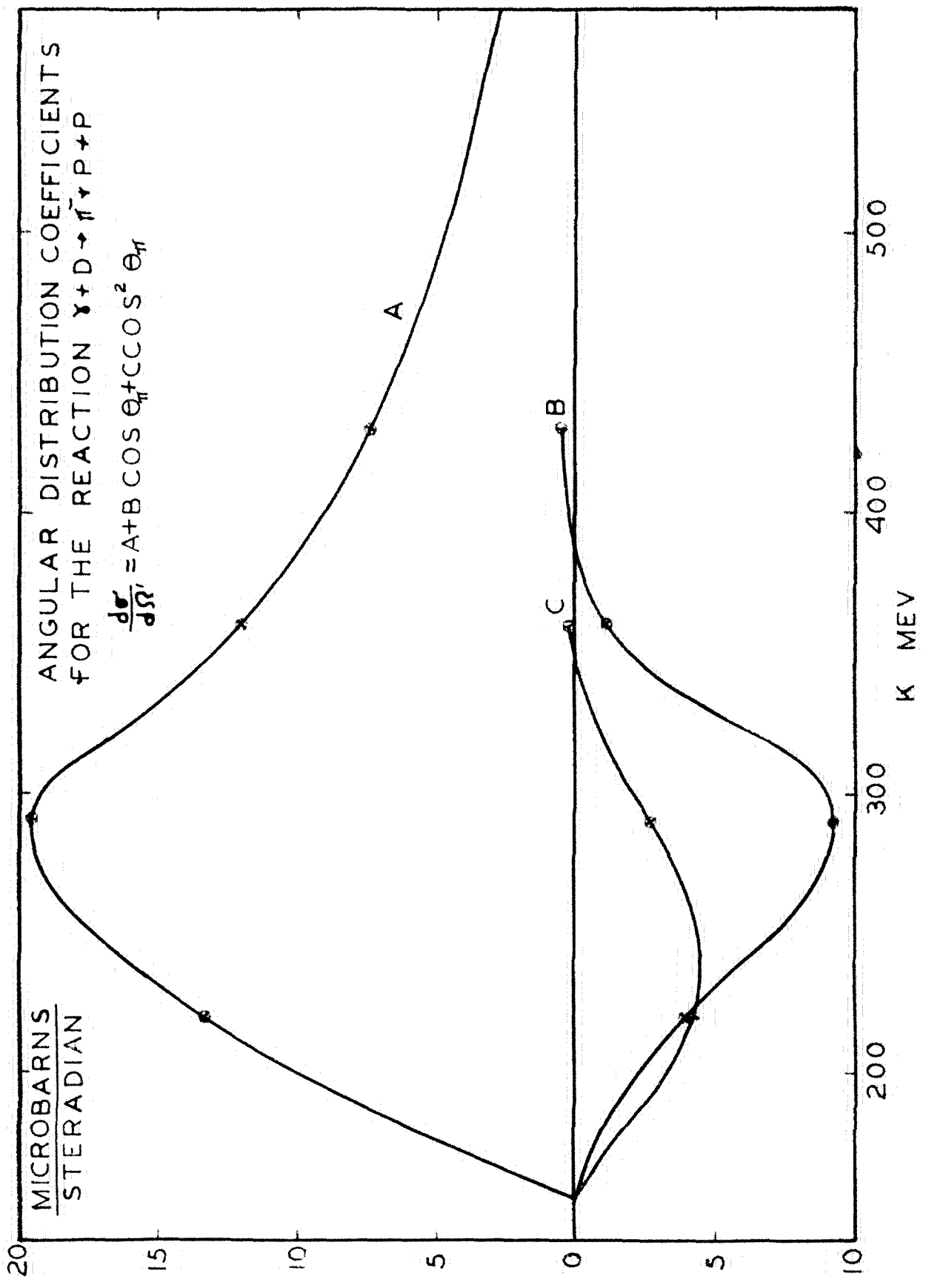
ANGULAR DISTRIBUTION COEFFICIENTS
FOR THE REACTION γ + D → π⁻ + P + P
dσ/dΩ' = A+B COS θπ+CCOS² θπ
A
B
C
MICROBARNS
STERADIAN
20
15
10
5
0
5
10
200
300
400
500
K MEV

Figure 27

The problem as previously outlined would be very lengthy by hand computation. The same equations must be solved two hundred times for each experimental point, of which there are twenty-one. However the problem was set up in this way with the intention of using the Datatron digital computer at the Jet Propulsion Laboratory. The Datatron did the computation in four or five hours computing time. The Datatron is an internally programmed computer with punched tape input and output. Its main memory has a capacity of 4,000 words (one word equals ten decimal digits and sign) and it has a rapid access memory of 80 words. Normal access time is 8.5 milliseconds and the rapid access time is .85 milliseconds. The computer program is introduced into the memory by punched tape. The machine will execute the instructions in sequence, unless one of the instructions is a change or a conditional change in the sequence. The instructions fall into two classes. The first class is the actual numerical computing. The second class is the data handling. The computing portion of the program will take the numbers in certain cells and perform various arithmetic operations on them, resulting in one or more answers. The data handling portion of the program must store these answers in the proper cells or punch them on tape, and select a new set of input numbers and store them in the calculation input cells and then switch control to the beginning of the calculation section. The data handling section makes all of the necessary decisions and stops the machine at the completion of the program. The program for this problem is illustrated by the flow diagram in figure 28. The box marked

FLOW DIAGRAM OF PART ONE OF THE CALCULATION

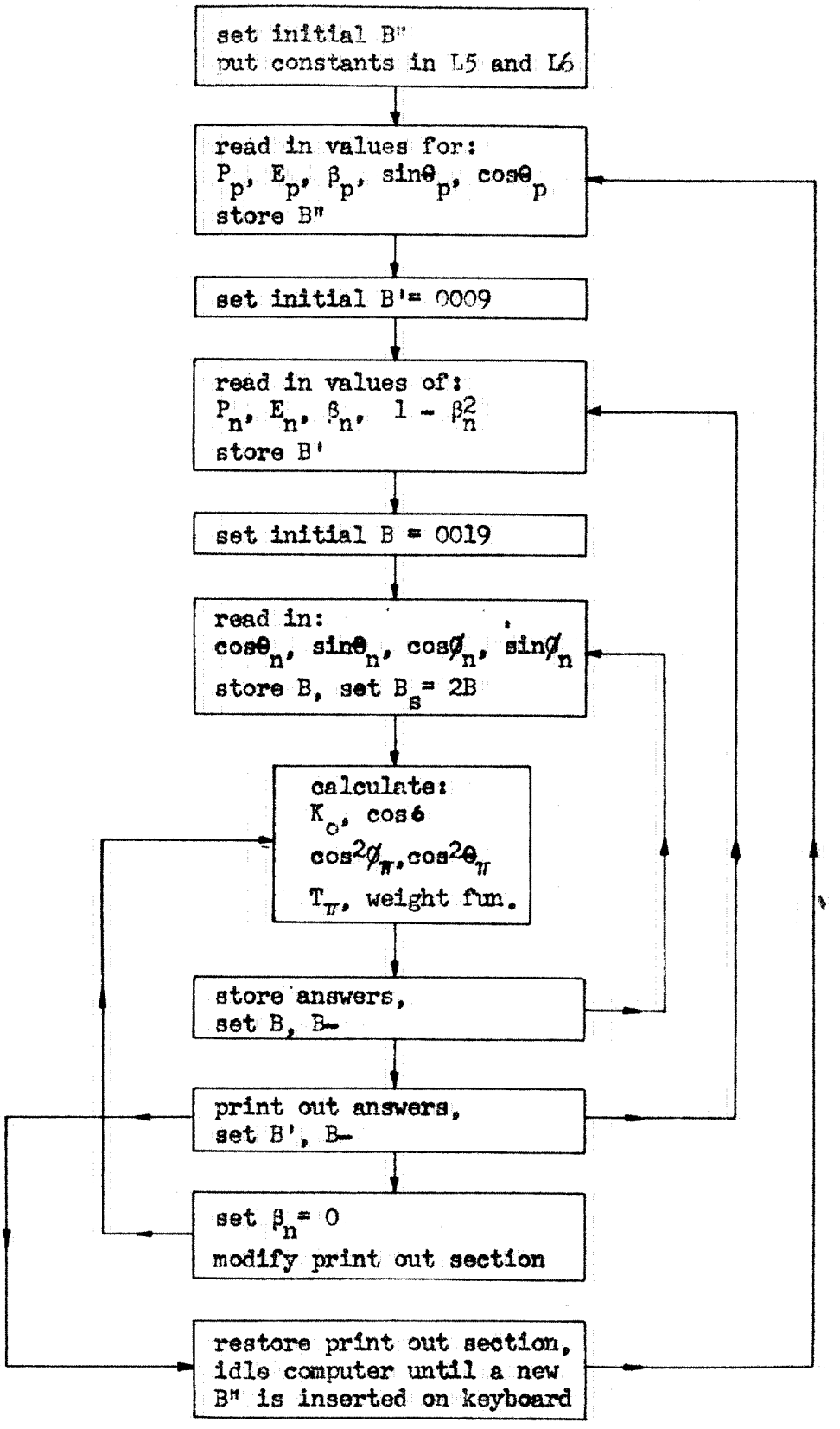

Figure 28

"calculate" contains all of the calculation and the rest of the diagram shows the data handling. In terms of time and number of instructions the "calculate" box contains the majority of the program, but it is quite straightforward. In order to understand the flow diagram it is necessary to know a little bit about the Datatron's B register. The B register can be controlled by regular machine instructions. It can be set to any number in the memory or its contents can be stored in the memory. The command B- on the flow chart means: if $B \neq 0$ subtract one from B and change control to the memory address contained in the B- command. If $B = 0$ go on to the next command in sequence. The B register can be used to control the number of times a sequence is repeated. The fact that B is reduced by one each circuit around the loop is also used in selecting the input data each time the loop is repeated.

This program uses the B register to control the three major loops. B'' is a number from 0 to 20 which determines which of the twenty-one telescope set up points is being calculated. At the end of a complete calculation for one telescope setting the Datatron will stop and two digits (the new B'') specifying the next point to be computed must be entered on the keyboard. It became apparent that not all of the points had to be calculated and considerable machine time was saved by doing only thirteen of the twenty-one points. B' has ten values corresponding to the ten values of momentum used in the problem. B has twenty values corresponding to the twenty possible directions of the momentum

of the target nucleon.

Part one of the program was actually the major part, about 80% of the total machine time. The result of part one was a punched tape with two hundred values of each of the following quantities: K_o, $\cos\delta$, the weighting function, $\cos^2\theta_\pi$, $\cos^2\phi_\pi$, and T_π. The first three quantities have been previously explained. The other three are the energy and direction of the meson. This output tape had two functions. It was run through the Flexowriter, (a tape controlled typewriter) which typed all of the information into a table. It was also used as an input tape for part two of the calculation which calculated the cross section at each point K_o, $\cos\delta$ and multiplied it by the weighting function and summed the contributions of the two hundred points. The cross section was stored in the memory of the Datatron by expanding it in the usual series:

$$\frac{d\sigma}{d\Omega'} = A + B\cos\delta + C\cos^2\delta.$$

The values of A, B, and C were stored in the memory for every even ten mev in K_o. To avoid the possibility of the machine getting a completely wrong answer when an occasional large K_o occurred, it was necessary to extrapolate the cross sections energies above the measured region before storing them in the machine. The contribution from the very high energy region is so small that the accuracy of the extrapolation is unimportant. The Datatron would start with a value of K_o and interpolate the coefficients and then calculate $\frac{d\sigma}{d\Omega'}$. By dividing the calculation into two parts

this way it was possible to change the cross sections used without having to do the major part of the calculation over again. The lower two boxes on the flow diagram are used to find the answers in the case where the target nucleon is at rest. This point can then be used as a reference to show the effect of the nucleon motions.

APPENDIX II

DERIVATION OF THE EQUATION FOR $\omega\bar{x}$.

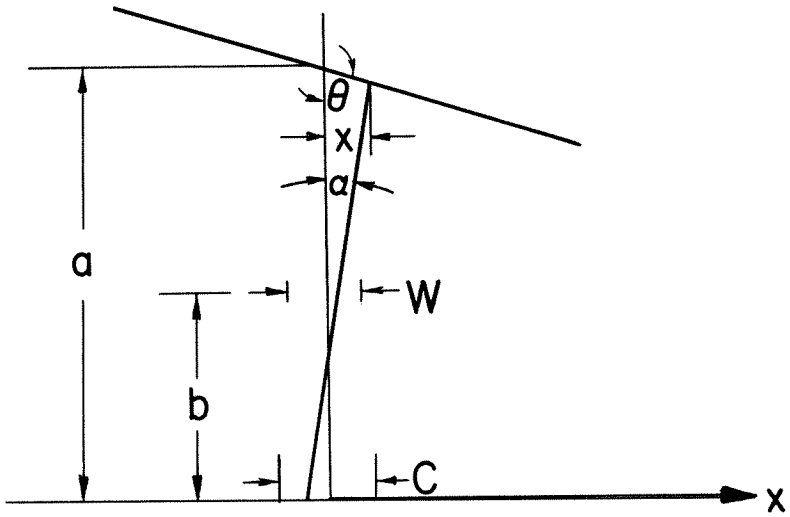

$\omega\bar{x}$ is the effective product of telescope solid angle and target length. The telescope consists of a counter of width C and height H, and a slit of width W separated a distance b. The counter is a distance a from the target, which is a line source at an angle θ with the telescope axis. The contribution to $\omega\bar{x}$ of an element of target ds is:

$\iint \frac{H}{r}\, d\alpha\, ds$, Where r is the distance from ds to the counter along a line making an angle α with the telescope axis. ds can be written $ds = \frac{dx}{\cos\theta}$. We may now write:

$$\omega\bar{x} = \frac{H}{\sin\theta} \iint \frac{1}{r}\, d\alpha\, dx,$$

where: $$r = \left(a - \frac{x}{\tan\theta}\right) \frac{1}{\cos\alpha},$$

and: $$\omega\bar{x} = \frac{H}{\cos\theta} \iint \frac{\cos\alpha}{a\tan\theta - x}\, d\alpha\, dx.$$

If we define $\omega\bar{x}^{+}$ as the contribution to $\omega\bar{x}$ from positive values of α, and similarly define $\omega\bar{x}^{-}$, then we have:

$$\omega\bar{x} = \omega\bar{x}^{+} + \omega\bar{x}^{-} = \omega\bar{x}^{+}(\theta) + \omega\bar{x}^{+}(\pi - \theta).$$

We will carry out the integration over x first. The limits are:

$$0 \leqslant \tan\alpha \leqslant \frac{C + W}{2b}; \quad x_{max} = \left(\frac{\tan\theta}{\tan\theta + \tan\alpha}\right)\left[\frac{W}{2} + (a - b)\tan\alpha\right],$$

$$0 \leqslant \tan\alpha \leqslant \frac{C - W}{2b}; \quad x_{min} = \left(\frac{\tan\theta}{\tan\theta + \tan\alpha}\right)\left[(a - b)\tan\alpha - \frac{W}{2}\right],$$

$$\frac{C - W}{2b} \leqslant \tan\alpha \leqslant \frac{C + W}{2b}; \quad x_{min} = \left(\frac{\tan\theta}{\tan\theta + \tan\alpha}\right)\left(a\tan\alpha - \frac{C}{2}\right).$$

After integrating and substituting limits we obtain:

$$\omega\bar{x}^{+} = \frac{H}{\cos\theta}\left\{\int_{0}^{\tan^{-1}\frac{C - W}{2b}} \cos\alpha \log\left(\frac{a\tan\theta + b\tan\alpha + \frac{W}{2}}{a\tan\theta + b\tan\alpha - \frac{W}{2}}\right) d\alpha \right.$$

$$\left. + \int_{\tan^{-1}\frac{C-W}{2b}}^{\tan^{-1}\frac{C+W}{2b}} \cos\alpha \log\left(\frac{a\tan\theta\,\frac{C}{2}}{a\tan\theta + b\tan\alpha - \frac{W}{2}}\right) d\alpha \right\}.$$

Since $b\tan\alpha$ is small compared to $a\tan\theta$, ($b\tan\alpha \leqslant W$) for the values of θ under consideration ($\theta \geqslant 30^{\circ}$) we rewrite the logarithm terms so that we may expand them. The constant logarithms may be immediately integrated:

$$\omega\bar{x}^{+} = \frac{H}{\cos\theta}\left\{\frac{c-w}{\sqrt{4b^2+(c-w)^2}}\ln\left(\frac{2a\tan\theta+w}{2a\tan\theta-w}\right)\right.$$

$$+\left(\frac{c+w}{\sqrt{4b^2+(c+w)^2}}-\frac{c-w}{\sqrt{4b^2+(c-w)^2}}\right)\ln\left(\frac{2a\tan\theta+c}{2a\tan\theta-w}\right)$$

$$\left.+\int_0^{\tan^{-1}\frac{c-w}{2b}}\cos\alpha\ln\left(1+\frac{2b\tan\alpha}{2a\tan\theta+w}\right)d\alpha-\int_0^{\tan^{-1}\frac{c+w}{2b}}\cos\alpha\ln\left(1+\frac{2b\tan\alpha}{2a\tan\theta-w}\right)d\alpha\right\}.$$

We now expand the logarithmic terms and integrate:

$$\int_0^{\tan^{-1}\frac{c-w}{2b}}\cos\alpha\ln\left(1+\frac{2b\tan\alpha}{2a\tan\theta+w}\right)d\alpha=\frac{2b}{2a\tan\theta+w}\left(1-\frac{2b}{\sqrt{4b^2+(c-w)^2}}\right)$$

$$-\frac{2b^2}{(2a\tan\theta+w)^2}\left(\ln\left[\tan\left(\frac{\pi}{4}+\frac{1}{2}\tan^{-1}\frac{c-w}{2b}\right)\right]-\frac{c-w}{\sqrt{4b^2+(c-w)^2}}\right)$$

$$+\frac{8b^3}{(2a\tan\theta+w)^3}\left(\frac{2b}{\sqrt{4b^2+(c-w)^2}}+\frac{\sqrt{4b^2+(c-w)^2}}{2b}-2\right)$$

+ higher order terms.

After integrating we write out the expression for $\omega\bar{x}^{-} = \omega\bar{x}^{+}(\pi-\theta)$ and add it to $\omega\bar{x}^{+}$ to obtain $\omega\bar{x}$:

$$\omega\bar{x}=\frac{H}{\sin\theta}\left\{\frac{2b^2}{a}\left(\frac{1}{1+x}+\frac{1}{1-x}\right)\left(\frac{1}{\sqrt{4b^2+(c+w)^2}}-\frac{1}{\sqrt{4b^2+(c-w)^2}}\right)+\frac{b^2x}{wa}\left(\frac{1}{(1-x)^2}-\frac{1}{(1+x)^2}\right)\right.$$

$$\left.\left(\ln\left[\tan\left(\frac{\pi}{4}+\frac{1}{2}\tan^{-1}\frac{c-w}{2b}\right)\right]-\frac{c-w}{\sqrt{4b^2+(c-w)^2}}+\ln\left[\tan\left(\frac{\pi}{4}+\frac{1}{2}\tan^{-1}\frac{c+w}{2b}\right)\right]-\frac{c+w}{\sqrt{4b^2+(c+w)^2}}\right)\right.$$

$$+\frac{2b^2X^2}{3W^2a}\left(\frac{1}{(1+X)^3}+\frac{1}{(1-X)^3}\right)\left(\frac{8b^2+(c-W)^2}{\sqrt{4b^2+(c-W)^2}}-\frac{8b^2+(c+W)^2}{\sqrt{4b^2+(c+W)^2}}\right)$$

$$+\frac{W}{2aX}\left(\frac{c+W}{\sqrt{4b^2+(c+W)^2}}+\frac{c-W}{\sqrt{4b^2+(c-W)^2}}\right)\ln\left(\frac{1+X}{1-X}\right)$$

$$+\frac{C}{2aY}\left(\frac{c+W}{\sqrt{4b^2+(c+W)^2}}+\frac{c-W}{\sqrt{4b^2+(c-W)^2}}\right)\ln\left(\frac{1+Y}{1-Y}\right)\Bigg\}.$$

Where the substitution $X = \frac{W}{2a\tan\theta}$, $Y = \frac{C}{2a\tan\theta}$ has been made.

We may abbreviate the coefficients as follows:

$$\omega\bar{X} = \frac{H}{\sin\theta}\left\{A\left(\frac{1}{1+X}+\frac{1}{1-X}\right)+BX\left(\frac{1}{(1-X)^2}-\frac{1}{(1+X)^2}\right)+CX^2\left(\frac{1}{(1+X)^3}+\frac{1}{(1-X)^3}\right)\right.$$
$$\left.+\frac{D}{X}\ln\left(\frac{1+X}{1-X}\right)+\frac{E}{Y}\ln\left(\frac{1+Y}{1-Y}\right)\right\}.$$

Expanding in X and Y we obtain:

$$\omega\bar{X} = \frac{H}{\sin\theta}\Big\{2A(1+X^2+X^4+\cdots)$$
$$+4B(\ X^2+2X^4+\cdots)$$
$$+2C(\ X^2+6X^4+\cdots)$$

(next term from log expansion gives only X^4 and higher terms)

$$+2D(1+\tfrac{1}{3}X^2+\tfrac{1}{5}X^4+\cdots)$$
$$+2E(1+\tfrac{1}{3}Y^2+\tfrac{1}{5}Y^4+\cdots)\Big\}.$$

$$\omega\bar{x} = \frac{2H}{\sin\theta}\left\{ \frac{2b^2}{a}\left(\frac{1}{\sqrt{4b^2+(c+w)^2}} - \frac{1}{\sqrt{4b^2+(c-w)^2}}\right)\right.$$

$$+ \frac{w}{2a}\left(\frac{c+w}{\sqrt{4b^2+(c+w)^2}} + \frac{c-w}{\sqrt{4b^2+(c-w)^2}}\right)$$

$$\left. + \frac{c}{2a}\left(\frac{c+w}{\sqrt{4b^2+(c+w)^2}} - \frac{c-w}{\sqrt{4b^2+(c-w)^2}}\right)\right\}$$

+ terms in X^2 and Y^2.

We now expand in $\frac{C+W}{2b}$ or $\frac{C-W}{2b}$ obtaining:

$$\omega\bar{x} = \frac{HCW}{ab\sin\theta} - \frac{Hb}{4a\sin\theta}\left[\left(\frac{C+W}{2b}\right)^4 - \left(\frac{C-W}{2b}\right)^4\right] + \text{terms in } X^2 \text{ and } Y^2.$$

$\omega\bar{x} = \frac{HCW}{ab\sin\theta}$ + error term. Since in our telescope $W \approx C$ we may estimate the error term by setting $W = C$, $X = Y$:

$$\text{Error} = -\frac{Hb}{4a\sin\theta}\left(\frac{W}{b}\right)^4 + \frac{2H}{\sin\theta}\left(A + 2B + C + \frac{1}{3}D + \frac{1}{3}E\right)X^2,$$

where:

$$A = \frac{b^2}{a}\left(\frac{1}{\sqrt{b^2+W^2}} - \frac{1}{b}\right) = \frac{b}{a}\left[-\frac{1}{2}\left(\frac{W}{b}\right)^2 + \cdots\right],$$

$$B = \frac{b^2}{Wa}\left\{\ln\left[\tan\left(\frac{\pi}{4} + \frac{1}{2}\tan^{-1}\frac{W}{b}\right)\right] - \frac{W}{\sqrt{b^2+W^2}}\right\} = \frac{b}{a}\left[\frac{1}{3}\left(\frac{W}{b}\right)^2 + \cdots\right],$$

$$C = \frac{2b^2}{3W^2a}\left(4b - \frac{4b^2+W^2}{\sqrt{b^2+W^2}}\right) = \frac{b}{a}\left[\left(\frac{W}{b}\right)^2 + \cdots\right]\left(-\frac{1}{3}\right),$$

$$D + E = \frac{W}{a}\frac{W}{\sqrt{b^2+W^2}} = \frac{b}{a}\left[\left(\frac{W}{b}\right)^2 + \cdots\right].$$

$A + 2B + C + \frac{1}{3}(D + E) = \frac{1}{6}\frac{b}{a}\left(\frac{W}{b}\right)^2$, so:

$$\text{Error} = -\frac{Hb}{4a\sin\theta}\left(\frac{W}{b}\right)^4 + \frac{2H}{\sin\theta}\,\frac{1}{6}\frac{b}{a}\left(\frac{W}{b}\right)^2\left(\frac{W}{2a\tan\theta}\right)^2.$$

We now obtain:

$$\omega\bar{x} = \frac{HCW}{ab\sin\theta}\left\{1 - \left[\left(\frac{W}{2b}\right)^2 - \frac{1}{3}\left(\frac{W}{2a\tan\theta}\right)^2\right]\right\}.$$

For the telescope used in this experiment the error term was 1/4000, which justifies using the simple expression:

$$\omega\bar{x} = \frac{AW}{ab\sin\theta}, \qquad \text{where } A = HC = \text{area of counter.}$$

CORRECTION FOR FINITE BEAM SIZE

The preceding derivation of $\omega\bar{x}$ was for the case of a line source. We now consider the effect of a beam of circular cross section and uniform intensity. We define the x direction to be the direction perpendicular to the beam in the plane containing the axis of the telescope and the axis of the beam. The normalized beam density is then:

$$I = \frac{2}{\pi R^2}\sqrt{R^2 - x^2}, \quad \text{where R is the radius of the beam.}$$

The effective $\omega\bar{x}$ will be obtained by integrating $\omega\bar{x}$ times the normalized beam intensity over the beam:

$$\overline{\omega\bar{x}} = \int_{-R}^{R} \omega\bar{x}\, I\, dx = \frac{2}{\pi R^2}\int_{-R}^{R} \sqrt{R^2 - x^2}\ \frac{AW}{b(a\sin\theta + x)}\ dx ,$$

We substitute $\sin\alpha = \frac{x}{R}$, $\cos\alpha = \sqrt{1 - \frac{x^2}{R^2}}$, $B = \frac{R}{a\sin\theta}$ obtaining:

$$\overline{\omega\bar{x}} = \frac{AW}{ab\sin\theta}\frac{2}{\pi}\int_{-\frac{\pi}{2}}^{\frac{\pi}{2}} \frac{\cos^2\alpha}{1 + B\sin\alpha}\, d\alpha ,$$

which may be rewritten:

$$\overline{\omega\bar{x}} = \frac{AW}{ab\sin\theta}\frac{2}{\pi}\left\{\frac{B^2-1}{B^3}\int_{-\frac{\pi}{2}}^{\frac{\pi}{2}} \frac{d\alpha}{\frac{1}{B} + \sin\alpha} + \frac{1}{B^2}\int_{-\frac{\pi}{2}}^{\frac{\pi}{2}} (1 - B\sin\alpha)\, d\alpha\right\}.$$

Using Dwight 859.21 to integrate we obtain:

$$\overline{\omega\bar{x}} = \frac{AW}{ab\sin\theta}\frac{2}{\pi}\left\{\frac{B^2-1}{B^3}\frac{\pi}{\sqrt{\frac{1}{B^2} - 1}} + \frac{\pi}{B}\right\} = \frac{AW}{ab\sin\theta}\,\frac{2 - 2\sqrt{1 - B^2}}{B^2} .$$

Expanding $\sqrt{1 - B^2}$ and substituting for B, we find:

$$\overline{\omega x} = \frac{AW}{ab\sin\theta}\left[1 + \frac{1}{4}\left(\frac{R}{a\sin\theta}\right)^2 + \cdots\right].$$

For the telescope used in this experiment and the beam diameter employed this correction term is less than 1/2000.

REFERENCES

(1) Photoproduction of Neutral Mesons in Hydrogen: Magnetic Analysis of Recoil Protons
D. C. Oakley and R. L. Walker
The Physical Review vol. 97, p. 1283 (1955)

(2) The Scattering of High Energy Neutrons by Nuclei
S. Fernbach, R. Serber, and T. B. Taylor
The Physical Review vol. 75, p. 1352 (1949)

(3) The Cross Section for Star Production in Nuclear Emulsions by 130 mev Protons
C. F. Lees, G. C. Morrison, H. Muirhead and W. G. V. Rosser
Philosophical Magazine vol. 44, p. 304 (1953)

(4) M. P. Ernstene, A. V. Tollestrup, and J. C. Keck
Private communication

(5) Photoproduction of Pi Meson Pairs
R. E. Cutkosky and F. Zachariasen
The Physical Review vol. 103, p. 1108 (1956)

(6) Negative-to-Positive Ratio of Photomesons from Deuterium
Matthew Sands, J. G. Teasdale, and Robert L. Walker
The Physical Review vol. 95, p. 592 (1954)

(7) Two-Nucleon Potential from the Cut-Off Yukawa Theory
Solomon Gartenhaus
The Physical Review vol. 100, p. 900 (1955)

(8) Photoproduction of Neutral Pions from Hydrogen at Foreward Angles from 250 to 500 mev
Dale Corson, V. Z. Peterson, and W. S. McDonald
To be published

(9) Low-Energy Photoproduction of π^o Mesons from Hydrogen: Total Cross Section
F. E. Mills and L. J. Koester, Jr.
The Physical Review vol. 98, p. 210 (1955)

(10) Photodissociation of the Deuteron from 150 to 450 mev
J. C. Keck and A. V. Tollestrup
The Physical Review vol. 101, p. 360 (1956)

(11) Photodisintegration of Deuterium by 60 to 250 mev X-Rays
E. A. Whalin, Barbara Dwight Schriever, and A. O. Hanson
The Physical Review vol. 101, p. 377 (1956)

(12) Ratio of Positive Photomesons from Deuterium and Hydrogen
M. Sands, J. G. Teasdale, R. L. Walker, R. Querzoli and M. A. Bloch
To be published

(13) The Range and Straggling of Protons between 35 and 120 mev.
N. Bloembergen and P. J. Van Heerden
The Physical Review vol. 83, p. 561 (1951)

(14) Production of Photomesons in Deuterium
James Keck and Raphael Littauer
The Physical Review vol. 88, p. 139(L) (1952)

(15) James Keck
Private communication

(16) The Interaction of High Energy Neutrons and Heavy Nuclei
M. L. Goldberger
The Physical Review vol. 74, p. 1269 (1948)

(17) High Energy Particles page 347
Bruno Rossi
Prentice-Hall, Inc. (1952)

(18) Partial Wave Analysis of the Experimental Photomeson Cross Sections
K. M. Watson, J. C. Keck, A. V. Tollestrup and R. L. Walker
The Physical Review vol. 101, p. 1159 (1956)

(19) Elastic Photoproduction of π^{o} Mesons from Deuterium
B. Wolfe, A. Silverman and J. W. De Wire
The Physical Review vol. 99, p. 268 (1955)

(20) Elastic Photoproduction of π^{o} Mesons from Deuterium
J. W. Rosengren and N. Baron
The Physical Review vol. 101, p. 410 (1956)

(21) Transition Curves of 330 mev Bremsstrahlung
Wade Blocker, Robert W. Kenney and Wolfgang K. H. Panofsky
The Physical Review vol. 79, p. 419 (1950)

(22) D. H. Cooper, Thesis, California Institute of Technology (1955)

(23) Photoproduction of Neutral Mesons in Hydrogen at High Energies
R. L. Walker, D. C. Oakley, and A. V. Tollestrup
The Physical Review vol. 89, p. 1301 (1953)

(24) Photodisintegration of the Deuteron by Meson Reabsorption
Robert R. Wilson
The Physical Review vol. 104, p. 218 (1956)

(25) Charged Photomesons from Various Nuclei

Raphael M. Littauer and Darcy Walker

The Physical Review vol. 86, p. 838 (1952)

(26) Photoproduction of Charged Pi Mesons from Hydrogen and Deuterium

T. L. Jenkins, D. Luckey, T. R. Palfrey and R. R. Wilson

The Physical Review vol. 95, p. 179 (1954)

(27) Photomeson Production from Deuterium

I. L. Lebow, B. T. Field, D. H. Frisch and L. S. Osborne

The Physical Review vol. 85, p. 681 (1952)

(28) π^+ Photoproduction Ratio of Deuterium to Hydrogen

K. M. Crowe, R. M. Friedman, and D. C. Hagerman

The Physical Review vol. 100, p. 1799 (1955)

(29) The Production of Charged Photomesons from Deuterium and Hydrogen

R. S. White, M. J. Jakobson and A. G. Schulz

The Physical Review vol. 88, p. 836 (1952)

(30) Production of π^o Mesons in Hydrogen and Deuterium by High Energy γ Rays

G. Cocconi and A. Silverman

The Physical Review vol. 88, p. 1230 (1952)

(31) Neutral Pion Production in Deuterium and Hydrogen: Ratios

J. C. Keck, A. V. Tollestrup, and H. H. Bingham

The Physical Review vol. 103, p. 1549 (1956)